The Search for Planets around Pulsating White Dwarf Stars

by

Fergal Mullally, B.Sc.

THESIS

Presented to the Faculty of the Graduate School of

The University of Texas at Austin

in Partial Fulfillment

of the Requirements

for the Degree of

MASTER OF ARTS

THE UNIVERSITY OF TEXAS AT AUSTIN

August 2003

The Search for Planets around Pulsating White Dwarf Stars

APPROVED BY

SUPERVISING COMMITTEE:

D. E. Winget, Supervisor

T. von Hippel

To St. Jude, the patron saint of lost causes.

And to Arthur Guinness, for his timely, but all too infrequent reminders of the better things in life.

Acknowledgments

The concept of individual work in modern scientific research is something of a misnomer, Newton's idea of progress being based on "standing on the shoulders of giants" has never been more apt. There are many people whose individual efforts have been vital to the continuation of this project. I would not consider it inappropriate to replace my name as author of this work with a list of everyone I know.

First among those whose efforts deserve recognition is my advisor, Don Winget, who first conceived of this novel method of searching for planets and also Ed Nather who built the image acquisition instrument and software vital for this work. I would also like to extend my gratitude to Ted von Hippel who has been a constant source of practical advice on everything from how to use UNIX to how to get the most from a PhD. Neither would this work have been possible without the unceasing efforts of the staff at McDonald Observatory, and especially Dave Doss, who have suffered most from my efforts to grow from student to astronomer.

I would like to thank the graduate students and postdocs of the department for making my stay here so enjoyable, and also my roommate, Andrew Kenna, for consenting to live in the disaster zone that was our apartment for the last 6 months. Finally, I would like to thank Susan Thompson for her invaluable support and assistance during the preparation of this manuscript.

The Search for Planets around Pulsating White Dwarf Stars

Fergal Mullally, M.A.
The University of Texas at Austin, 2003

Supervisor: D. E. Winget

We present a new method for searching for planets around other stars with a different sensitivity to other methods by using the pulsations of white dwarf stars as stable clocks. Finding planets around other stars is the first step toward establishing the existence and abundance of life around other stars in the universe. It has broader implications for star formation, planet formation, stellar evolution and even biology. Most stars will eventually become white dwarf stars so we will be able to sample a wide range of stellar ages and types. Theoretical predictions generally agree that the red giant phase of stellar evolution will consume the inner planets of a stellar system, but leave planets further out intact. Our method preferentially detects those planets at larger radii.

A subset of pulsating white dwarf stars have pulsational stability that exceeds most pulsars and rivals that of atomic clocks. When a planet is in orbit around a star the reflex orbital motion of the star will produce a detectable change in arrival time of the pulses which is linearly dependent on both the mass and orbital separation of the planet.

Before searching for planets we first increased the number of suitable stars from 8 to 22, by searching for suitable candidates in the Sloan Digital Sky Survey. We also present results from archival data on two stars which rule out the possibility of Jupiter or Saturn like planets around these stars.

Table of Contents

List of Tables

List of Figures

Chapter 1

Introduction

1.1 Background

The discovery of a planet around 51 Peg (Mayor & Queloz, 1995) created a surge in interest in searching for planetary companions of other stars. At the time of writing, there are 117 claimed planet detections, although as yet only a handful have been confirmed by an independent detection method. The discovery of extra-solar planets is the first step in determining the presence and frequency of life in the universe. Study of other planetary systems also gives insight into the formation of our own solar system.

A white dwarf (WD) is believed to form as the remnant of a main sequence star after the red giant phase. All stars with an initial mass less than 8 $M_{\odot}$ are believed to form WDs. WDs are typically about $0.6M_{\odot}$, squeezed into a volume about the size of the earth. At this high density the electrons are highly degenerate. Significant nuclear burning has ceased; the evolution of the star is one of simple cooling from an initial temperature of approx $150,000K$. The distribution of temperatures of WDs can be used to place a lower bound on age of the Galaxy (Winget et al., 1987)

DAVs are DA type (hydrogen atmosphere) white dwarf stars that pulsate in an instability strip $1,500K$ wide around $12,000K$. The V in the designation stands for variable (Sion et al., 1983). A subset of these pulsators, known has hot DAVS, or HDAVs, exhibit extreme stability in period and phase

of their oscillations. The method of pulsation is consistent with non-radial g-modes.

The simplest method of stellar oscillation to understand is radial pulsation, where the outer layers of the star become opaque to radiation and are heated. They rise, cool, become transparent and fall back down again. The extremely high gravity in WDs makes vertical motion difficult, and instead the oscillation drives motion along gravitational equipotential surfaces. The oscillations cause temperature variations on the surface of the star that can be described by spherical harmonic functions. The increase in temperature causes an increase in emitted flux, while there is a corresponding decrease in flux from cooler parts of the surface. To an observer this manifests itself as a time varying luminosity change.

The period of pulsation of a given mode is governed by the radius and temperature of the oscillator (Winget (1998) and references therein). As these objects are highly degenerate their radius is effectively constant, so the change in pulsation period is determined by the slow, predictable cooling of the star (Mestel, 1952). The drift in period is uni-directional and has been measured at 3.4×10^{-15} for G117-B15A (Kepler et al., 2000), accounting for proper motion, and constrained to less than 5.5×10^{-15} in the case of R548 (Mukadam et al., 2003a). This class of star constitutes one of the most stable objects known, with stability greater than most pulsars and rivalling that of atomic clocks.

By far the most popular and successful method to search for planets is the radial velocity method which favours bright, nearby, main sequence stars of similar spectral type to our own sun. Searching for planets around white dwarf stars opens up an entirely new planet parameter space to investigation. White dwarf progenitors span a wide range on spectral type when on the main

sequence. As stars of different spectral type have different lifetimes, from hundreds of millions to billions of years, we can determine planet formation rates at different periods of Galactic evolution. Most importantly, the search for planets around pulsating WDs is more sensitive to planets at larger radii, and can comfortably detect Jupiter mass at $5AU$, where theorists (e.g Boss (1995)) suggest that gas giant planets should form.

1.2 Will Planets Survive the Red Giant Phase?

1.2.1 Theory

All WDs were once main sequence stars and therefore potential hosts for planetary systems. However, before becoming a WD a star passes through the red giant phase, typically losing of order a solar mass of material in the process. This mass loss, coupled with the very strong solar wind that would accompany it, presents a threat to the stability of an orbiting planet. During the Red Giant phase the star's atmosphere will expand 100 – 200 times before the nuclear burning ceases.

Livio & Soker (1984) attempted to calculate the behaviour of a planet at $454R_{\odot}$ (about $1AU$) during the red giant phase. They found that a low mass planet would spiral into the star and evaporate but suggested that above a critical mass the planet would accrete matter and evolve into very short period companion of the parent star.

Rasio et al. (1996) contend that the earth would be consumed by the sun as it entered the red giant phase, Debes & Sigurdsson (2002) set the limit for orbital stability at $5AU$ for the initial semi-major axis.

Soker (1994) showed that the planetary orbits would expand roughly adiabatically during the mass loss phase but the effect of tidal forces would be to reduce the size of the final semi-major axis.

Burleigh et al. (2002) noting that large stars lose more than half their mass before becoming WDs worried that this is sufficient, if lost instantaneously, to cause the planet's orbit to be energetically unstable against escape, but concluded that the most rapid mass loss phase occurred over a period of 10^4 years which was very much longer than the orbital time of most planets, hence planetary stability should not be affected in this way.

Duncan & Lissauer (1998) performed numerical simulations of the stability of multi-planet systems while the star is losing mass and for 1 billion years afterwead. They found that planets were stable for at least this period of time, which is long enough for the WD to cool to the DAV instability strip.

The consensus is that the innermost planets inside $\sim 1AU$ will be consumed by the Red Giant, but planets further out will have their orbits perturbed but remain in the system.

However, these models have yet to be tested against observation, which is what we intend to do. If we do not find planets with large masses and long period orbits, this may mean the planets were indeed lost during the the mass loss phase of the red giant, information which can be used to improve our models of red giants and the interactions between winds and planets.

1.2.2 Observation

Observationally, we have two pieces of evidence which increase our confidence that planets do survive the Red Giant phase. First is the infrared excess

from the pulsating white dwarf G29-38 (Zuckerman & Becklin, 1987) which could be due to a brown dwarf companion. The second is the recent discovery by of a planet around the K Giant ι Draconis (Frink et al., 2002), which strengthens the case that Red Giants don't necessarily destroy planets.

1.3 Expected Success Rate

Based on the success of the radial velocity method in discovering planets we can hope to estimate the frequency of planets around WDs. However such an effort is fraught with unknowns and should be approached with utmost caution. As previously stated, white dwarf progenitors span a wide range of spectral types, initial masses, metallicities, formation age and distance away from us.[1] Radial velocity planets, on the other hand, are predominantly metal rich F or G type stars in the solar neighbourhood. Metal rich stars have more stellar lines which improves the accuracy of the velocity measurement. Stars of the same type in the same region of the Galaxy can be expected to have a small spread in masses, metallicites and formation age. We must also worry that the radial velocity method favours the detection of close in planets while we will preferentially find planets that are further out, and predict the loss of the close in planets during the Red Giant phase.

Bearing in mind these uncertainties, we can still attempt to make a rough estimate of the number of planets that we might find. Assuming for a moment that all planets will survive the red giant phase, we expect the fraction of WDs that have Jupiter mass planets to be roughly equal to f_p,

[1]For example, a 19th magnitude white dwarf would be typically ≈ 700 parsecs away, while a G type star with an apparent magnitude of 8 would be 36 parsecs away (8th magnitude is about the faintest star that can be used for high resolution radial velocity work).

the fraction of main sequence stars with Jupiter mass planets. Lineweaver & Grether (2003) sets the success rate of the radial velocity method as $9\% \pm 3\%$ for stars monitored for ~ 13 years[2]. Based on the radial velocity method, we can empirically set $f_p = 0.1$, taking no account of the different biases in that survey as opposed to our own.

However, we do note that the radial velocity method is most sensitive to planets in close in orbits. Planet formation theories (Boss, 1995) suggest that these giant planets do not form close to their parent star, but form further out and some drift inward due to interactions with remaining disk material. This would suggest that our empirical f_p is a lower bound on the true value. Further, Lineweaver & Grether (2003) show that more planets are being found further out than closer in, again arguing that our f_p is a lower bound. On the other hand, most of the planets discovered thus far will be destroyed when their parent star becomes red Giant, suggesting that we should use f_p as an upper bound. When faced with unmeasured effects such as these, the best thing to do is to ignore them, but treat the result with skepticism. We therefore claim that in the case of WDs, $f_p = 0.1$, unchanged from the empirical result of the radial velocity surveys. So if we search 30 WDs, we expect to find 3 stars with planetary companions, although we should not be at all surprised if the success rate is very different.

Even if we are correct that the frequency of planetary systems around WDs is 10%, it is unlikely that a search of 30 stars will reveal exactly 3

[2]Calculating the success rate of the radial velocity method, which is being undertaken by many different groups at many different sensitivities, is no trivial matter. Lineweaver & Grether (2003) gives the raw success rate as 5% of stars surveyed have planets, 9% of Sun-like stars have planets with $M \sin i > 0.3 M_{Jupiter}$, $P < 13$years and $\sim 21\%$ for $M \sin i > 0.1 M_{Jupiter}$, $P < 60$years.

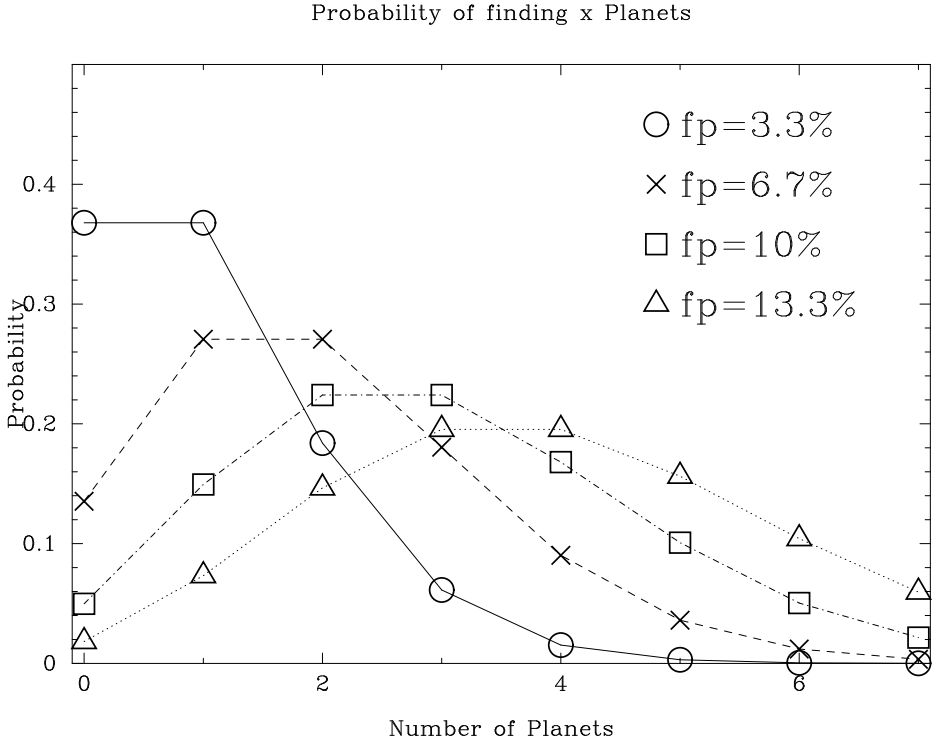

Figure 1.1 Poisson distribution of expected number of planets found around 30 stars for different values of f_p. For $f_p = 10\%$, there is a 5% chance that we will discover no planets at all in our sample. The reader is reminded that any estimates for f_p should be treated with skepticism.

planetary systems. We might get lucky and find one or two more, or unlucky and find one or two less. Because we expect to be dealing with a rare event (i.e finding a planetary system), we can model our expected success rate as a Poisson distribution (Bevington (1969), Sec. 2.2). If we search n stars with an expected frequency of planetary systems f_p, we should expect, on average, to find $\mu = nf_p$ systems.[3] In the limit of $\mu \ll 1$, the probability of finding

[3]In Bevington (1969) the probability of success is denoted by p. In our case the probability of success is the frequency of planetary systems, f_p. We choose to keep our notation

exactly x systems can be expressed as

$$P = \frac{\mu^x}{x!} e^{-\mu} \tag{1.1}$$

Fig. 1.1 shows this distribution for a number of different values of f_p. The square symbols correspond to $f_p = 10\%$, or an average of 3 systems in 30 stars.

1.4 Physics of Finding Planets

When a star has a planetary companion, both objects orbit their mutual center of mass. The distance from the center of mass of the star to the center of mass of the system is given by the equation

$$a_* = \frac{ma}{M + m} \tag{1.2}$$

where a_* is the distance from center of mass of star to center of mass of system, a is the distance from the center of mass of the planet to the center of mass of the system, which is almost equal to the semi major axis of orbit of the planet, m is the mass of the planet and M is the mass of the star.

As the star and planet complete a full orbit, the star is alternatively closer and then further away from the observer depending on the phase of the orbit. This distance is modulated by the sine of the inclination angle i between the plane of the orbit and the line of sight of the observer. Because light travels at a constant speed in a vacuum, the time of arrival of photons

consistent with the rest of this document rather than with our source.

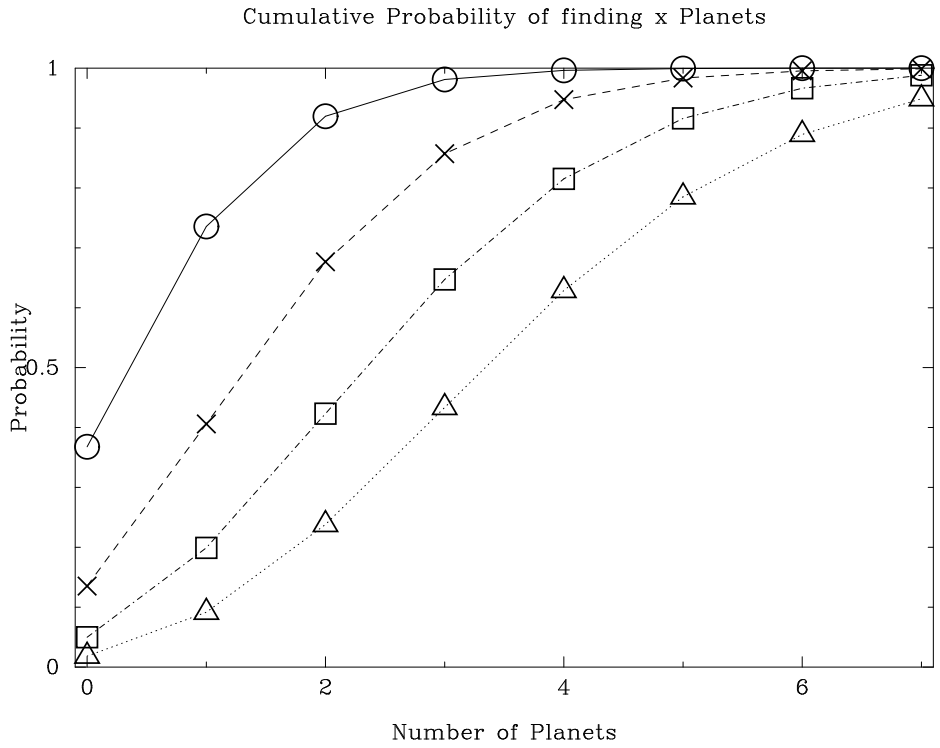

Figure 1.2 Cumulative expected success rate for a sample of 30 stars and different values of f_p. Each point represents the probability of discovering x or fewer planets. The symbols are the same as Fig 1.1. We can see that for a survey of 30 HDAVs, we have a $> 90\%$ probability of finding one or more planets for $f_p = 8\%$. For $f_p = 10\%$ the probability of finding no planets is 5% and the probability of finding at least 3 planets is of order 65%. The lines are drawn for clarity, the probability of discovering an non-integer number of systems is, of course, undefined.

emitted by the star as observed on the earth changes over a full orbit by an amount equal to

$$2\frac{a_* \sin i}{c} = 2\frac{ma \sin i}{(M+m)c} \tag{1.3}$$

where c is the speed of light.

In the limit of companion mass $\ll$ stellar mass, this equation simplifies to

$$\tau = \frac{ma \sin i}{Mc} \tag{1.4}$$

where τ is the semi-amplitude of the change in light travel time. The key point to note from this equation is that our ability to detect a planet increases linearly with both the mass and orbital separation of the planet. The further away the planet is from the star, the larger the change in arrival time. This allows us to search a different region of parameter space than the radial velocity method.

For a Jupiter mass planet at $5.2AU$ around a $0.55M_{\odot}$ white dwarf, $\tau = 5$ seconds. The change in arrival time of the photons will be detected as a change in the observed phase of the pulsations.

In order to detect the presence of a planet by this method, we must observe stars that are emitting a regular signal with a period or phase jitter less than the size of the signal we are trying to detect. As previously mentioned in Section 1.1, HDAVs are the most stable optical clocks known making them ideal for this search

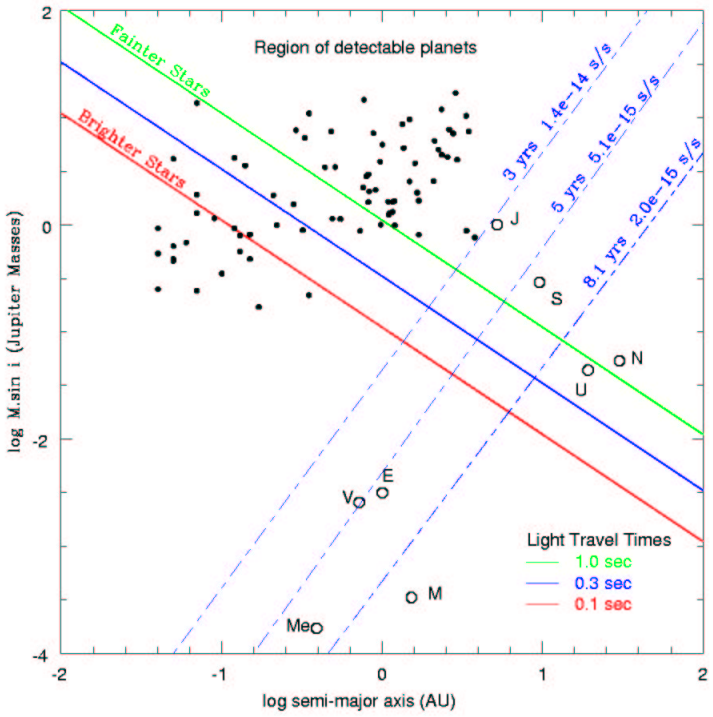

Figure 1.3 Projected planet detection limits. The open circles are planets in our own solar system. The dots are planets discovered by the radial velocity method. The solid lines are planet detection limits for different noise limits between 1–0.1 seconds. The dashed lines are the limits we will be able to place on long period companions and the time it will take us to reach those limits. Plot taken from Mullally et al. (2003)

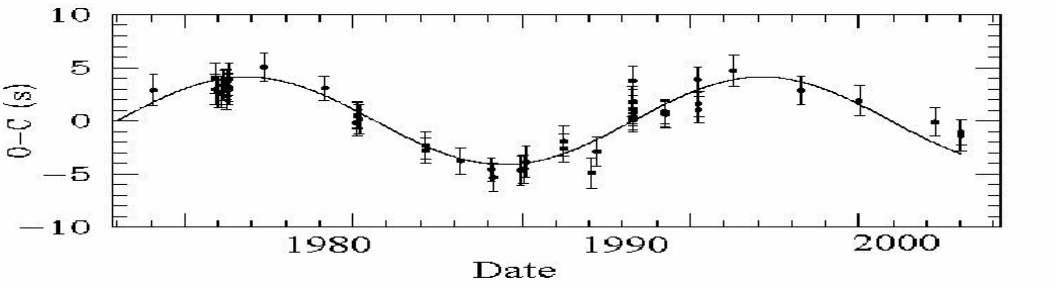

Figure 1.4 Simulated planet around a previously known HDAV, G117-B15A. The parabola in the O-C diagram due to evolutionary cooling was removed from data previously recorded from the past 25 years and the effect of a Jupiter mass planet at 5.2AU was superimposed. The effect of Jupiter is unquestionable.

1.5 Measurement of Period Drift Constrains Presence of Long Period Planets

Measurement of the drift in period places further constraints on the presence of planets in long period orbits. The observed pulsational period of a star will change slightly as it is accelerated in its orbit due to a planetary companion. For a long period orbit, we can collect enough data to measure this small acceleration. The change in period, $\dot{P}_{plan}$ due to an orbital companion, is given by

$$\dot{P}_{plan} = \frac{P}{c}\frac{Gm\sin i}{a} \tag{1.5}$$

where G is Newton's constant of gravitation, m is the mass of the planet, i is the inclination angle, a is the orbital separation, and c is the speed of light (Kepler et al., 1991). If we measure a drift in period consistent with the cooling of the star we can place strong limits on the presence of large orbital period companions.

A planet in a large orbit will cause a very large change in pulse arrival times over a very long period corresponding to the orbital period of the planet. However given a long enough time, the small change in pulsation period due to the acceleration if the star in its orbit can be measured. The change in observed period will be seen as a drift in observed pulse arrival time. Measuring the drift in arrival time due to the changing period (itself due to the cooling of the star) we can place limits on planets in long period orbits.

Measurement of the drift in pulse arrival time due to cooling of the star also yields information on the physics of the star's internal composition. If a star has no orbiting companions, then the slow change in period due to cooling will be measurable. As described in Kepler et al. (1991), the rate of cooling depends on the elemental composition of the stars core (the amount of Helium, Carbon and Oxygen, etc.). The measured $\dot{P}$ can be compared to theoretical estimates to determine the composition.

The limits on $\dot{P}$ improve with the square of the time that the star is monitored, as the measured value of the delay between the observed time of arrival of a pulse and that expected based on a constant period, $O - C$, is given by

$$O - C = \Delta E_0 + \Delta P E + \frac{1}{2} P \dot{P} E^2 \tag{1.6}$$

where E is the Epoch, ΔE_0 is the difference between the start of the first epoch and its measured value, and ΔP is the difference between the period and it's measured value. For more details consult Kepler et al. (2000) and Kepler et al. (1991).The limits on long period planets are measured from the curvature in the best fit parabola to $O - C$. The deviation of $O - C$ from a straight line increases with the square of the epoch.

Chapter 2

Discovering new HDAVs

2.1 Why do we want more HDAVs?

Searching for a planet around one star is an interesting demonstration of an observational technique. To learn something about the distribution of planets around WDs as a class, we need to look at a much larger sample of stars. Taking the naive estimate of f_p of 10% from the introduction, we can expect to find three planets if we examine 30 stars, and ten planets if we observe 100 stars. The results presented in the chapter will be published in Mukadam et al. (2003c).

The first pulsating white dwarf, HL Tau 76, was discovered by accident by Landolt (1968). G117-B15A, the first HDAV was discovered by Richer & Ulrych (1974). As of 2001 there were 8 known HDAVs (see Table 2.1).

As described in Mukadam et al. (2003c), Greenstein (1982) acquired

Star Name	Magnitude	Star Name	Magnitude
G117-B15A	15.54	L19-2	13.75
R548	14.16	G226-29	12.5
G185-32	12.98	GD165	11.4
G238-53	15.5	GD244	16.0

Table 2.1 Previously Known HDAVs, from Bradley (1993), except GD244 from Fontaine et al. (2001)

multichannel spectrophotometry for 14 DAVs, and found that they lie in a narrow range in color space $-0.41 \leq G - R \leq -0.29$. He concluded that the narrow band $(G - R)$ color is an excellent temperature indicator for DAs. Others, such as McGraw et al. (1981) found no constant stars in this region. Fontaine et al. (1982) showed that DAV candidate selection based on the Johnson filter system (more similar to the filter system used by the SDSS) yields a 30% success rate for discovering new ZZ Ceti stars, from a sample of spectroscopically identified DA white dwarfs. Hence we expected to find one pulsator for every 3 candidates observed at the telescope and started using the photometric technique in the initial stages of the project.

2.2 The source of our new variables

The Sloan Digital Sky Survey (SDSS) (York et al., 2000) ambitiously attempts to catalogue and obtain 5 colour photometry of every object down to 23th magnitude over one quarter of the entire sky. At the time of writing, they estimate that they will complete 65% of this target within the period for which they are currently funded.

We can estimate the number of HDAVs we expect to find in the Sloan survey based on the number of DAVs uncovered in previous surveys of this type. The PG survey (which covers an identical area of sky to the Sloan Survey) found a surface density of DAs of 0.19 per square degree of sky down to a magnitude of $B = 17.5$, (Homeier et al. (1998) and Fan (1999)) of which 0.0538 were DAVs.

Homeier et al. (1998), compared overlapping fields in the PG survey and the Hamburg Schmidt survey and concluded that the PG survey underestimated the surface density of DAs by a factor of 50%. This implies that the

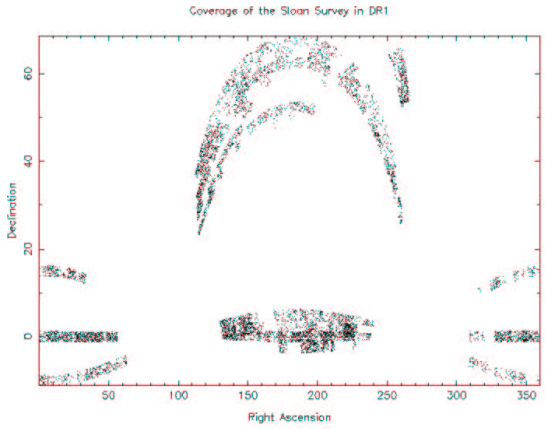

Figure 2.1 Sky coverage of the Sloan survey available at time of writing. Each point represents the position of an object with a spectrum and colours close to that of a DAV.

true surface density of DAVs is 0.0153 down to $B = 17.5$.

With our new CCD photometer, Argos (Nather & Mukadam, 2003), we can find pulsators down to a magnitude of 19.5. This extra 2 magnitudes allows us to detect DAVs 2.5 times further away, allowing us probe a volume of space 6.3 times greater than we could at 17.5. This extra depth will increase the surface density of DAVs on the sky to .0968 per square degree, assuming a constant white dwarf space density out to this distance.

If completed, the Sloan survey will survey $10,000$ square degrees of sky, and in doing so should uncover 968 DAVs down to 19.5. Of the DAVs currently known, one in three is a HDAV, so we expected about 320 HDAVs to be found by the Sloan. This number will have to be modified by the fraction of the planned area that the Sloan actually completes.

We had originally hoped to discover the necessary number of WDs by examining the broad band SDSS colours (Fukugita et al., 1996) to determine

whether an object lay within the pulsation instability strip of DA WDs, then performing high speed photometric observations on it to determine whether or not it pulsated. Based on previous experience (see above) we were confident of achieving a success rate of at least one in three, however our success rate was closer to one in ten.

So why was our success rate so low? The answer can be seen in Fig 2.2 below. The grid-lines are adapted from Bergeron et al. (2001) and show the colours of DA WDs of different temperatures and gravities. As previously stated the width of the instability strip is approximately $1500K$, but the scatter in this plot is very much greater. Indeed, the scatter is very much greater than the quoted $1\% - 2\%$ precision (Smith et al., 2002). The pulsators therefore spill over into the non-pulsating region, and non-pulsators contaminate the instability strip.

2.3 Using Spectral Information

For a number of objects, the Sloan also provides medium resolution spectra. Although the primary focus of the Sloan Survey is extragalactic objects, they also take spectra of interesting stellar objects. The similarity of WDs and quasars in their broad band photometric colours also have helped increase our sample of WDs with Sloan spectra. Two methods were used to the determine whether a given object with a spectrum was a candidate pulsator.

The first, implemented by our collaborators Kleinmann & Nitta at Apache Point Observatory, fits the spectra to atmosphere models developed by Detlev Koester (Koester et al., 1994).

The second measures the equivalent widths of the dominant absorption

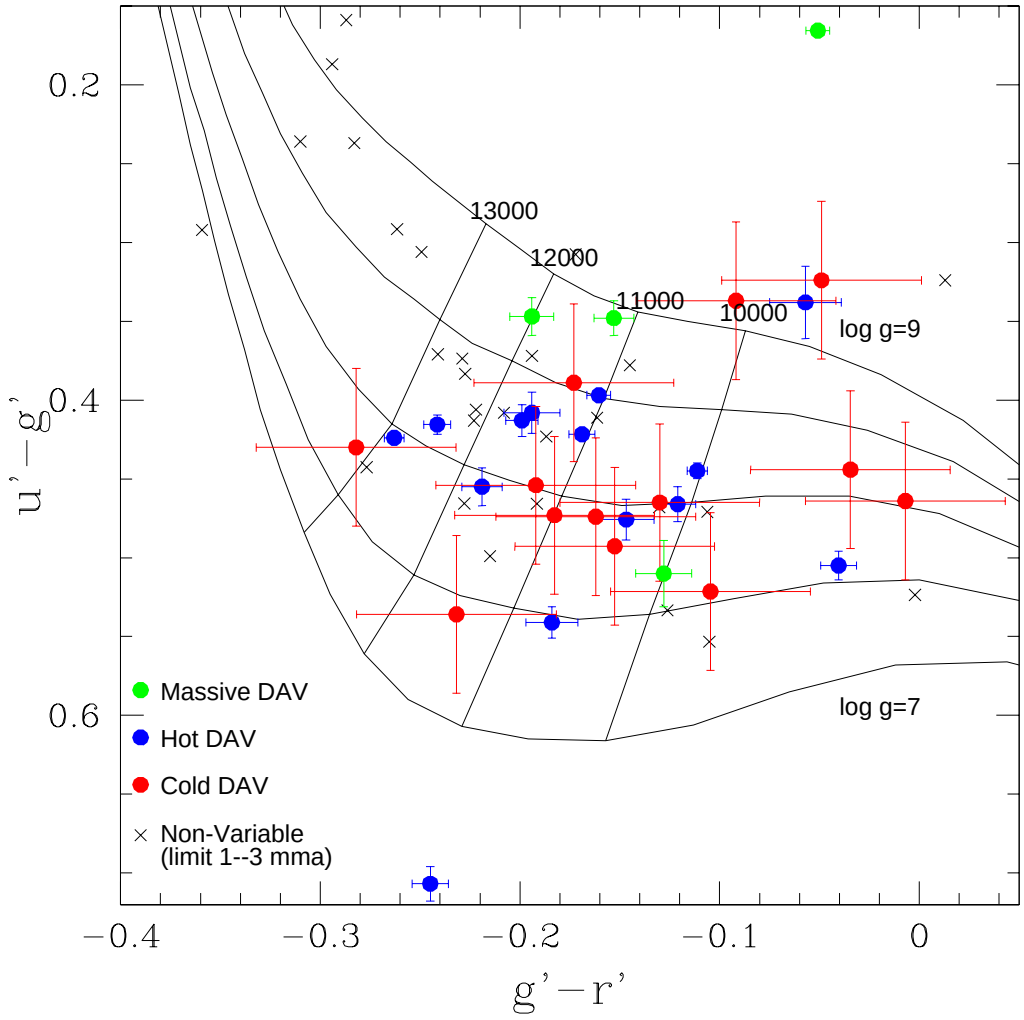

Figure 2.2 Pulsators and non-pulsators in Sloan colour space. The grid of temperatures and log(g) is taken from Bergeron et al. (2001). The pulsators are distributed of an area of colour space far wider than the expected $1500K$. Plot courtesy A. Mukadam.

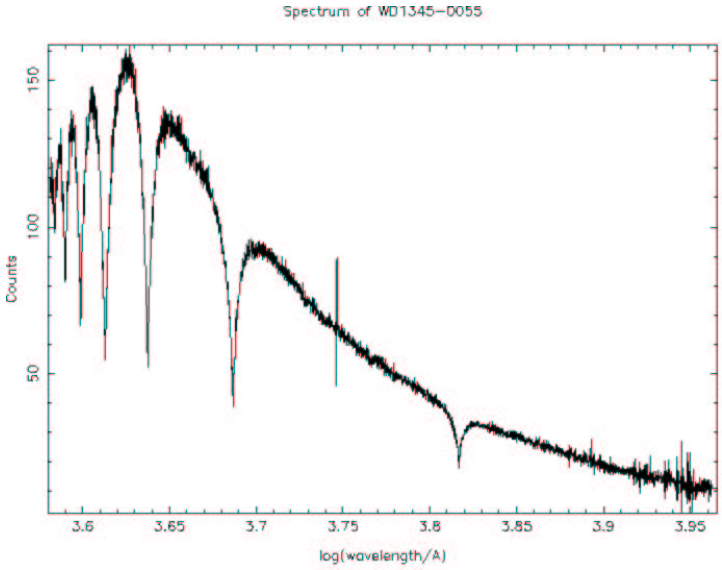

Figure 2.3 Optical spectrum of a typical HDAV take from the Sloan survey. This particular specimen is spSpec-51666-0300-288, corresponding to the pulsator WD1345-0055. This spectrum is of particularly good quality as WD1345 is so bright (16.7). The wavelength scale is logarithmic, the Sloan convention. The blue end of is approximately $3900\mathring{A}$, the red edge is close to $9000\mathring{A}$. The Balmer lines caused by atmospheric hydrogen are by far the most dominant feature.

lines, comparing them to the equivalent widths of known pulsators. The dominant absorption lines in the optical region of the spectrum of WDs are the Balmer absorption series, pressure broadened by the extremely high gravity. The equivalent widths of the H_β and H_γ lines correlate well with the temperature and gravity of the star which, it is believed, uniquely determine whether or not the star pulsates (Fontaine et al. (1985), Bergeron et al. (1995)). The advantage of this method is that one does not need to calculate the expected equivalent width of the Balmer lines of a pulsator, but merely measure it from previously discovered WDs. In simple terms, if the measured equivalent widths of the lines of a candidate star are close to the equivalent widths of previously discovered pulsators, it is then a good candidate to observe to determine whether it pulsates. The disadvantage of this method is that there isn't a unique temperature solution for a given ratio of equivalent widths. As the temperature of the star falls, the equivalent widths of the Balmer lines rise until a maximum $13,500K$ (Fontaine et al., 2003). At this point they begin to fall again. Therefore objects at temperatures around $12,000K$ are indistinguishable from others around $15,000K$. For this reason, we can, at best, hope for a 50% success rate from this method, unless we incorporate our colour information, which we have not yet done. This degeneracy also affected the fitting technique which up until recently did not use the colour information either to differentiate between potential pulsators and non-pulsators.

For reasons as yet unexplained, the success of each of these methods individually is quite poor. However, when an object is selected by both methods as likely to be a pulsator, the success rate rises to 12 in 24 or 50%. Of these, half have light curves consistent with stable pulsators, half are consistent with unstable pulsators. Of our non-pulsators, many were observed under non-ideal

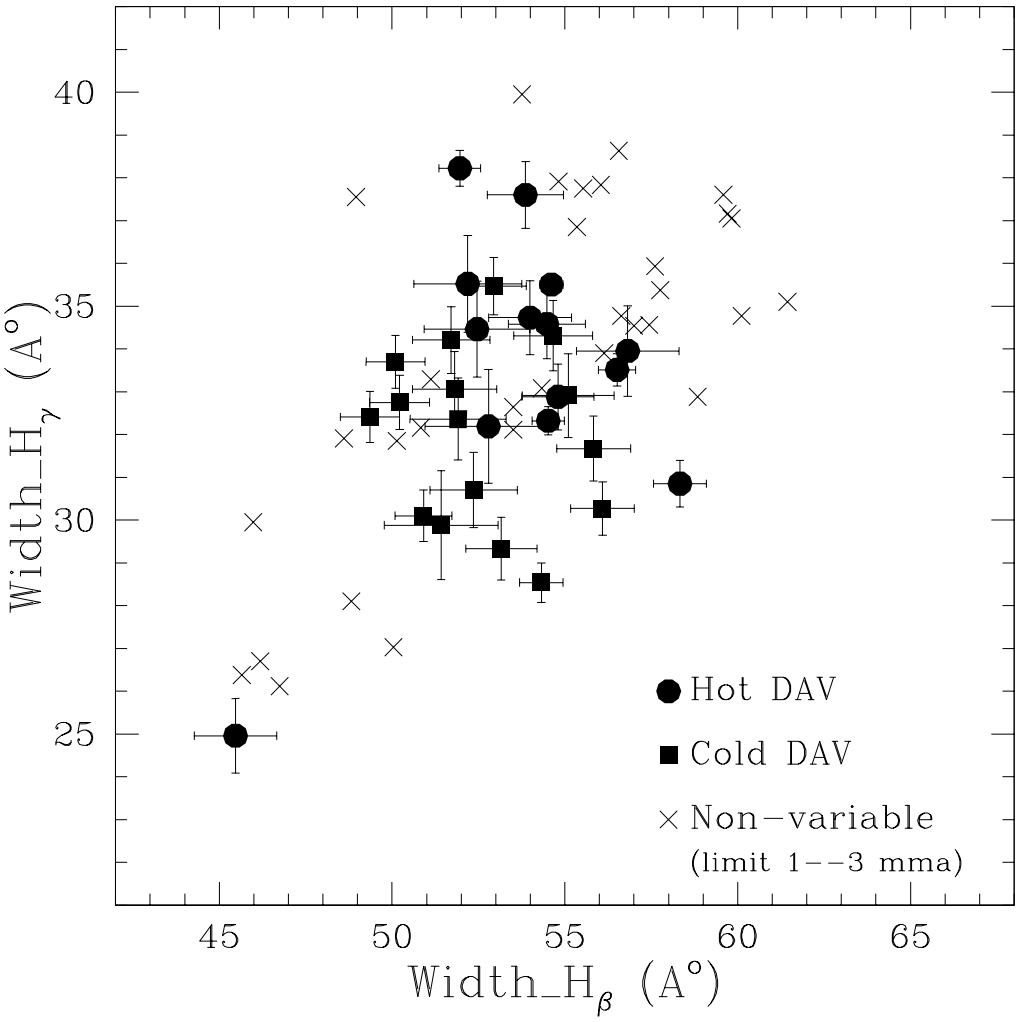

Figure 2.4 Equivalent widths of the H_β and H_γ lines of pulsators and non-pulsators. The dots indicate stable pulsators, the squares are unstable pulsators unsuitable for planet searches and the crosses are stars which were observed to not pulsate at a limit of better than 0.3%. There is a general trend of stable pulsators having larger equivalent widths than unstable pulsators. Plot from Mukadam et al. (2003c)

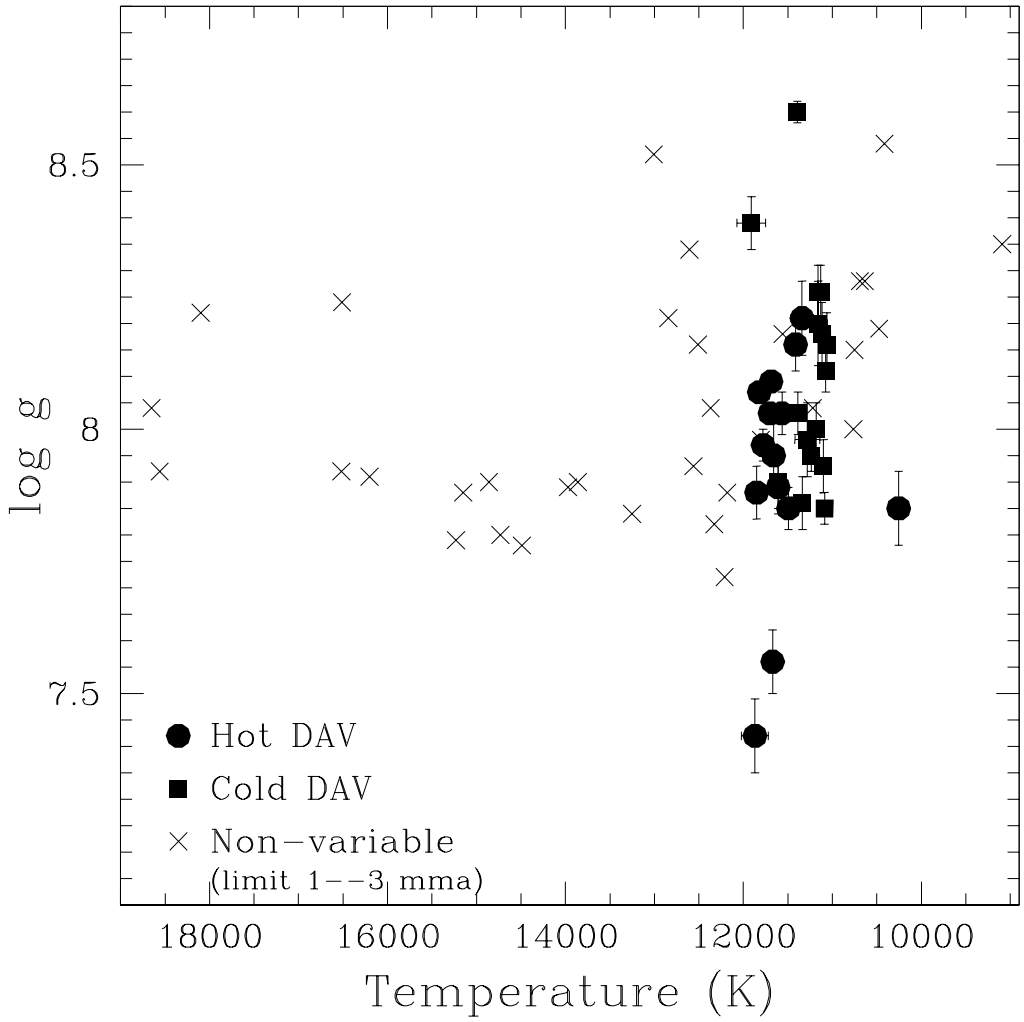

Figure 2.5 Temperature and gravities of pulsators and non-pulsators based on fits to their spectra. The dots are stable pulsators, the squares are unstable pulsators unsuitable for planet searches and the crosses are stars which were observed to not pulsate at a limit of better that 0.3%. The purity of the strip and the separation between stable and unstable pulsators contrasts starkly with the poor separation in colour space in Fig 2.2. Plot from Mukadam et al. (2003c)

weather conditions, giving poor non-variable limits of around 0.5%. Although we can not classify these stars as non-pulsators, we do not re-observe them under better conditions as pulsators with amplitudes below 0.5% are unsuitable for our planet search. Ignoring these stars improves our success rate to 80%. We therefore claim a 80% success rate under good conditions, and a 50% success rate under all conditions.

2.4 Results

As of May 2003 we have discovered 32 new pulsating WDs from the Sloan survey. These discoveries are published in Mukadam et al. (2003c) and are reproduced in Table 1.2 & 1.3. The following figures show the Fourier Transforms of the light curves of these pulsators.

2.5 Future Work

Of these 32 pulsators discovered in the Sloan survey, 15 are of the stable HDAV variety. This brings the total number of HDAVs observable in the northern hemisphere to 22 (L19-2 has a declination of 81 degrees south). This means that 8 additional HDAV pulsators need to be discovered for the first phase of this project. Each candidate star is observed for two hours to determine whether it pulsates, and confirmed with a second 4 hour run if it is a HDAV. Given our success rate of approximately 25% for finding HDAVs, 12 hours of observing, or approximately 1.5 nights are required to discover and confirm a HDAV. We estimate that it will take 12 nights of clear observing to discover the remaining HDAVs.

Table 2.2. New ZZ Ceti variables

Object	Plate	MJD	Fiber	RA_{2000}	Dec_{2000}	$T_{eff}(K)$	$logg$
WD0102−0032	396	51816	262	01:02:07	−00:32:59	11062 ± 90	8.16
WD0111+0018	694	52209	597	01:11:00	+00:18:07	11413 ± 90	8.16
WD0214−0823	668	52162	354	02:14:07	−08:23:18	11494 ± 79	7.85
WD0318+0030	413	51821	483	03:18:47	+00:30:29	11160 ± 67	8.26
WD0332−0049	415	51810	211	03:32:36	−00:49:18	11131 ± 69	8.26
WD0815+4437	547	51959	350	08:15:31	+44:37:10	11340 ± 130	8.21
WD0825+4119	760	52264	604	08:25:46	+41:19:00	11910 ± 160	8.39
WD0842+3707	864	52320	548	08:42:20	+37:07:01	11870 ± 150	7.42
WD0847+4510	763	52235	144	08:47:46	+45:10:06	11850 ± 110	7.88
WD0906−0024	470	51929	081	09:06:24	−00:24:28	11610 ± 86	7.90
WD0939+5609	556	51991	476	09:39:44	+56:09:40	11660 ± 110	7.95
WD0942+5733	452	51911	023	09:42:13	+57:33:42	11183 ± 60	8.00
WD0949−0000	266	51630	037	09:49:17	−00:00:23	11280 ± 140	7.98
WD0958+0130	500	51994	163	09:58:33	+01:30:49	11778 ± 55	7.97
WD1015+0306	503	51999	329	10:15:48	+03:06:48	11688 ± 33	8.09
WD1015+5954	559	52316	330	10:15:19	+59:54:30	11672 ± 92	7.56
WD1056−0006	276	51909	073	10:56:12	−00:06:21	11087 ± 51	7.85
WD1122+0358	836	52376	214	11:22:21	+03:58:22	11099 ± 78	7.93
WD1125+0345	836	52376	050	11:25:42	+03:45:06	11610 ± 100	7.89
WD1157+0553	841	52375	377	11:57:07	+05:53:03	11074 ± 49	8.11
WD1345−0055	300	51666	288	13:45:50	−00:55:36	11820 ± 53	8.07
WD1354+0108	301	51641	322	13:54:59	+01:08:19	11702 ± 46	8.03
WD1417+0058	304	51609	345	14:17:08	+00:58:27	11385 ± 80	8.03
WD1443+0134[2]	537	52027	279	14:43:30	+01:34:05	10430 ± 100	7.70
WD1502−0001	310	51990	229	15:02:07	−00:01:47	11116 ± 96	8.18
WD1524−0030[1]	...	...	...	15:24:03	−00:30:23	...	...
WD1617+4324	815	52374	390	16:17:37	+43:24:43	11336 ± 92	7.86
WD1700+3549	820	52433	110	17:00:55	+35:49:51	11237 ± 55	7.95
WD1711+6541	350	51691	362	17:11:13	+65:41:58	11392 ± 44	8.60
WD1724+5835	366	52017	264	17:24:28	+58:35:39	11565 ± 74	8.03
WD1732+5905	366	52017	591	17:32:35	+59:05:33	11160 ± 99	8.20
WD2350−0054	386	51788	135	23:50:40	−00:54:30	10254 ± 56	7.85

[1]WD1524−0030 does not have a spectrum; its object ID is 2255047396229223.

[2]The SDSS spectrum of WD1443+0134 shows only half of the H_γ line; its temperature and $\log g$ value may not be as reli able.

Stars in bold stable pulsators.

Table 2.3. New ZZ Ceti variables cont.

Width (H_β)	Width H_γ	Width (H_γ)	$u\prime$-$g\prime$	$g\prime$-$r\prime$	$g\prime$
WD0102−0032	54.66 ± 1.14	34.31 ± 0.82	0.43	−0.04	18.21
WD0111+0018	652.19 ± 1.56	35.52 ± 1.13	0.41	−0.19	18.76
WD0214−0823	54.80 ± 1.04	32.88 ± 0.77	0.28	−0.14	17.92
WD0318+0030	56.09 ± 0.92	30.27 ± 0.62	0.44	−0.18	17.81
WD0332−0049	53.16 ± 1.03	29.33 ± 0.73	0.42	−0.11	18.18
WD0815+4437	52.79 ± 1.83	32.19 ± 1.33	0.34	−0.06	19.30
WD0825+4119	55.10 ± 1.33	32.91 ± 0.98	0.34	−0.11	18.50
WD0842+3707	56.82 ± 1.48	33.95 ± 1.06	0.54	−0.18	18.75
WD0847+4510	53.99 ± 1.20	34.73 ± 0.86	0.42	−0.22	18.32
WD0906−0024	52.94 ± 0.95	35.47 ± 0.67	0.44	−0.18	17.73
WD0939+5609	52.46 ± 1.53	34.46 ± 1.12	0.43	−0.17	18.70
WD0942+5733	50.91 ± 0.82	30.10 ± 0.60	0.39	−0.13	17.43
WD0949−0000	51.42 ± 1.65	29.88 ± 1.27	0.45	−0.13	18.80
WD0958+0130	51.96 ± 0.60	38.22 ± 0.42	0.41	−0.23	16.70
WD1015+0306	54.61 ± 0.34	35.50 ± 0.24	0.37	−0.10	15.66
WD1015+5954	54.48 ± 1.11	34.58 ± 0.81	0.65	−0.31	17.95
WD1056−0006	49.36 ± 0.85	32.41 ± 0.60	0.15	−0.2	17.52
WD1122+0358	51.71 ± 1.12	34.21 ± 0.78	0.47	−0.01	18.13
WD1125+0345	53.86 ± 1.10	37.60 ± 0.78	0.46	−0.12	18.07
WD1157+0553	50.22 ± 0.87	32.75 ± 0.63	0.32	−0.04	17.59
WD1345−0055	56.51 ± 0.54	33.51 ± 0.38	0.38	−0.17	16.70
WD1354+0108	54.52 ± 0.47	32.32 ± 0.33	0.42	−0.17	16.36
WD1417+0058	55.83 ± 1.07	31.67 ± 0.76	0.47	−0.22	18.03
WD1443+0134	···	···	0.46	−0.12	18.72
WD1502−0001	52.36 ± 1.26	30.70 ± 0.88	0.37	−0.14	18.68
WD1524−0030	···	···	0.38	−0.23	16.03
WD1617+4324	51.81 ± 1.22	33.06 ± 0.88	0.45	−0.19	18.33
WD1700+3549	50.10 ± 0.85	33.70 ± 0.62	0.47	−0.16	17.26
WD1711+6541	54.32 ± 0.63	28.54 ± 0.46	0.19	−0.11	16.89
WD1724+5835	58.33 ± 0.77	30.85 ± 0.54	0.43	−0.19	17.54
WD1732+5905	51.91 ± 1.39	32.36 ± 0.96	0.47	−0.10	1 8.74
WD2350−0054	45.47 ± 1.19	24.96 ± 0.87	0.42	−0.11	18.10

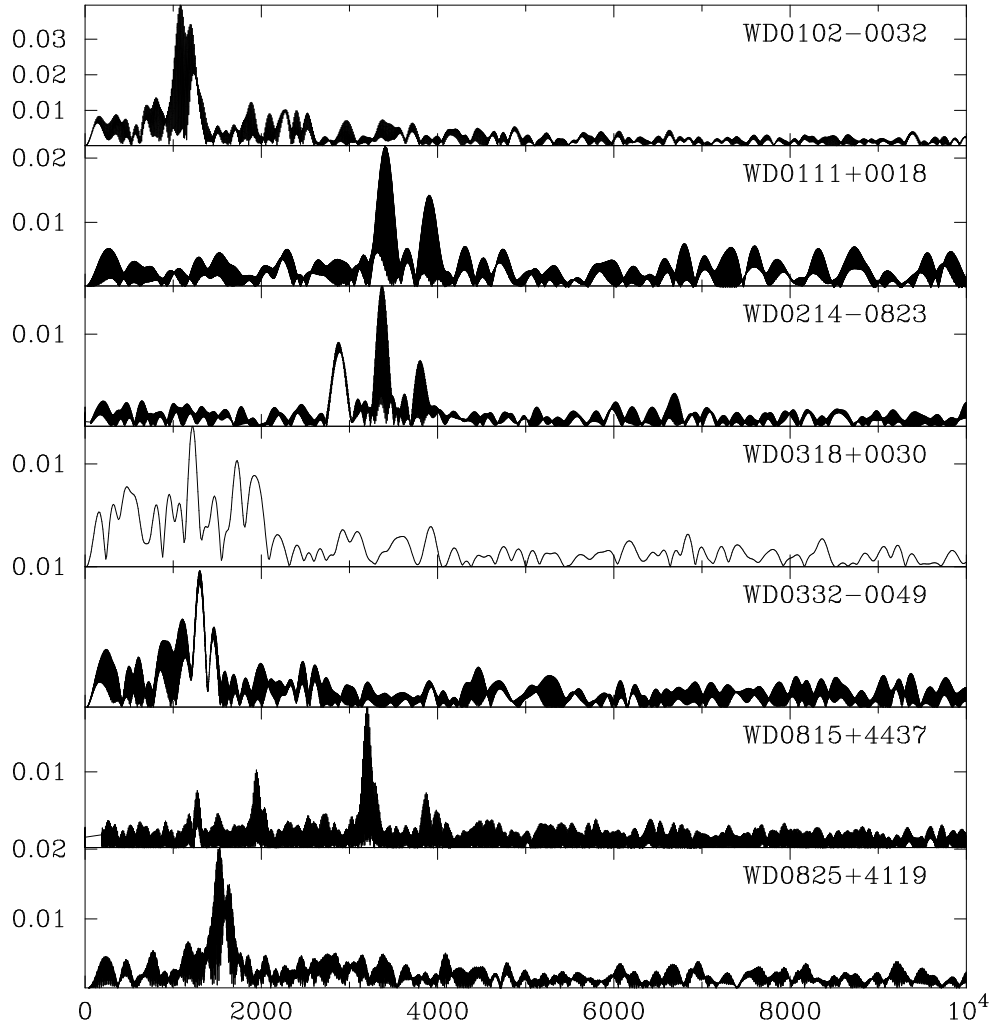

Figure 2.6 Fourier Transforms of pulsators discovered in the Sloan survey

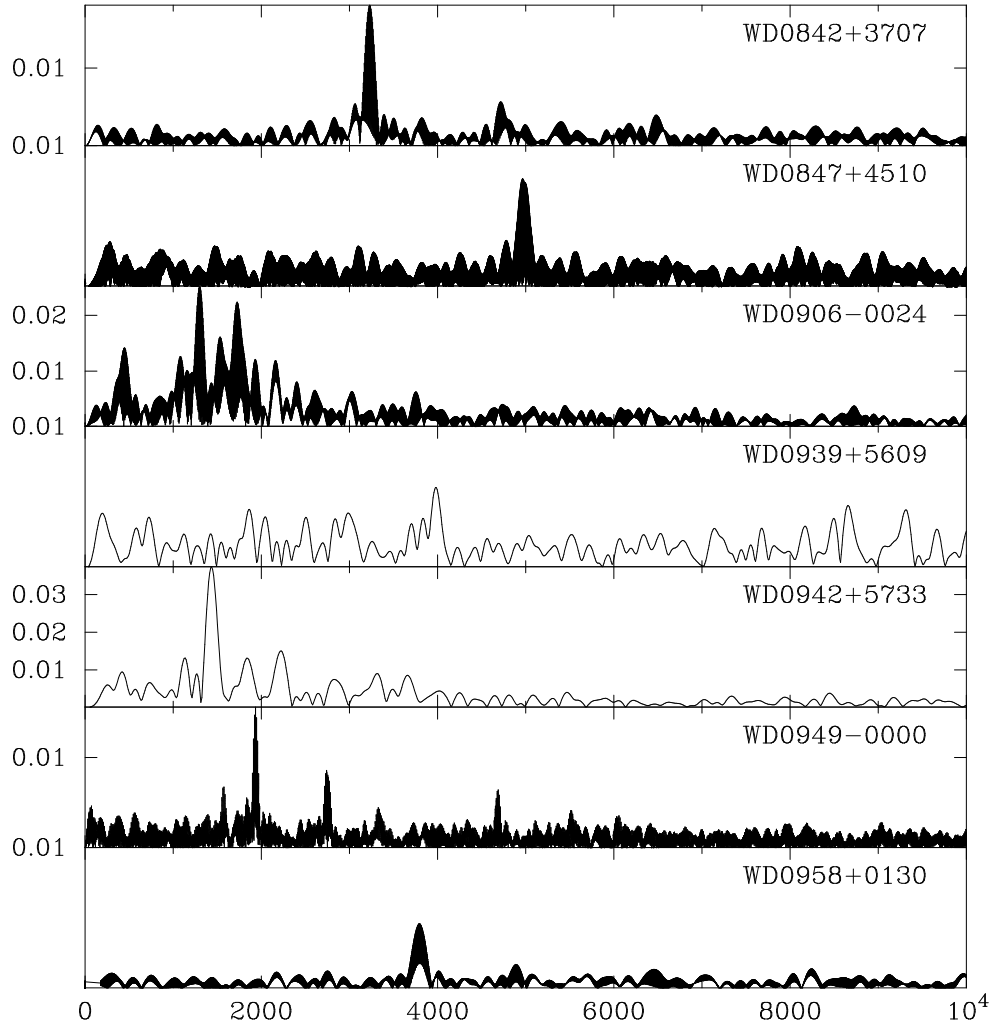

Figure 2.7 Fourier Transforms of pulsators discovered in the Sloan survey

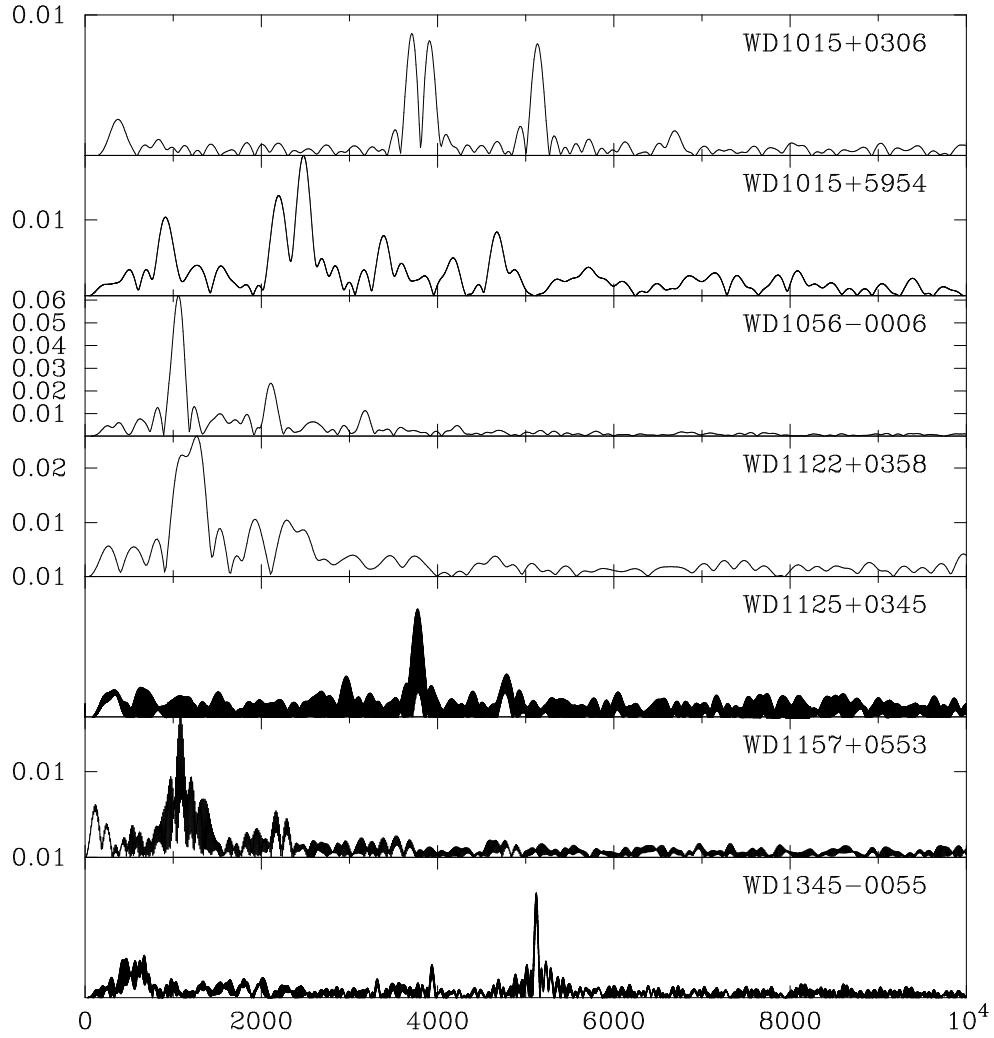

Figure 2.8 Fourier Transforms of pulsators discovered in the Sloan survey

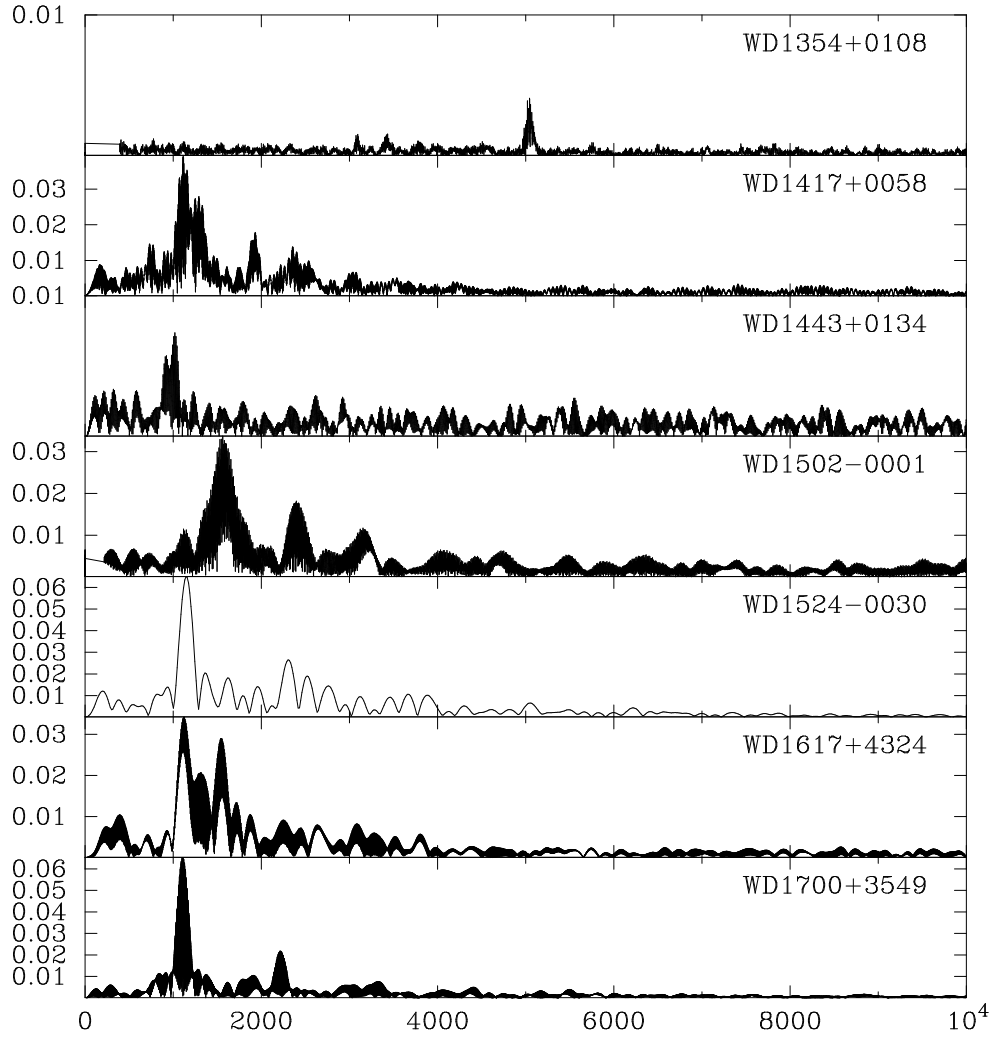

Figure 2.9 Fourier Transforms of pulsators discovered in the Sloan survey

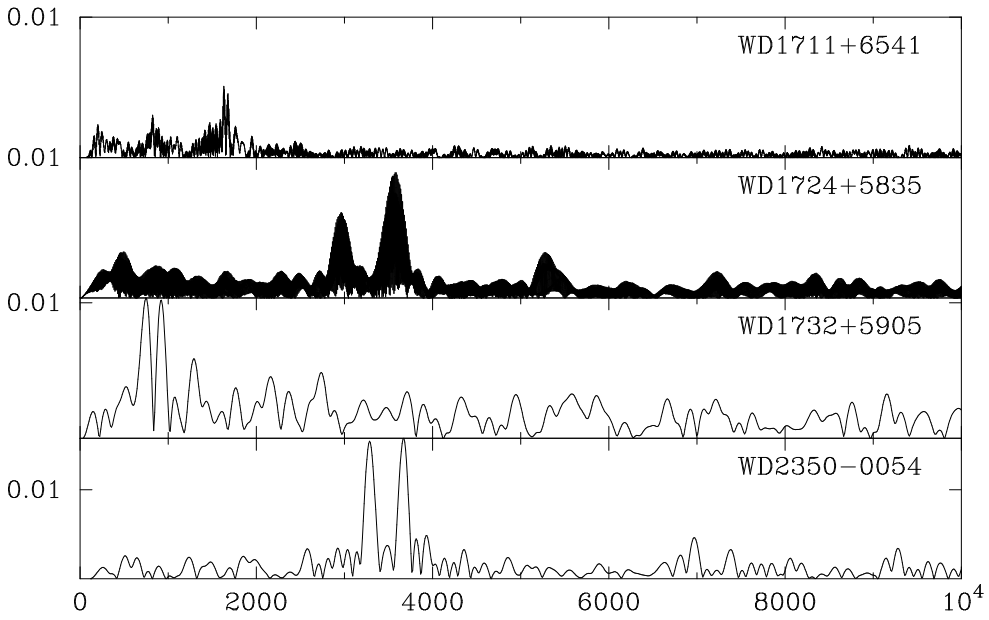

Figure 2.10 Fourier Transforms of pulsators discovered in the Sloan survey

Chapter 3

Data Analysis

3.1 Observation Technique

We observe stars with the Argos CCD prime focus photometer designed and built by Ed Nather (Nather & Mukadam, 2003), using the 2.1m Otto Struve telescope at McDonald Observatory. The core of this instrument is a Princeton Micromax 512 BFT NTE-CCD which has two characteristics which make it ideal for this work, blue sensitivity and a fast readout frame transfer buffer which means there is virtually no readout time.

The photometer takes a continuous series of images with exposures of 5 – 20 seconds of an area of sky 2.8 arcminutes on a side around a target star. The start time and duration of each exposure is tightly controlled by hardware connected to the GPS timing system.

Candidate pulsators are typically observed for 2 hours to determine if they pulsate. It is common practice when using CCDs to prepare the data by first flat-fielding each frame to correct for varying quantum efficiencies across the chip. However we have determined that our chip is sufficiently uniform that we will not mis-classify any star by not flat-fielding our data.

The software that runs Argos, Quilt 11, includes a real time light curve extraction routine, however we have found it unsuitable for use for moderately dim stars, or moderately poor observing conditions. Instead, light curves

are currently extracted from the frames using a routine written by Antonio Kanaan, which is based on IRAF's DAOPHOT. This routine is not satisfactory for our work as it frequently, and seemingly randomly, loses stars on frames or produces sudden jumps in the number of counts which are unrelated to any apparent changes in the images. Part of the future work of this project is to find or write more robust image analysis software.

After extraction, the target star's lightcurve, a sum of a selection of target stars and a measurement of sky are converted to Quilt 9 format for analysis with the Quilt EDit program (QED). QED was designed for use with the 3 channel PMT photometers (Kleinman et al., 1996) and can only accommodate one reference star. This is not suitable to our needs, but is sufficient to find new pulsators. Because CCD photometry provides us with sky subtracted counts with many fewer artefacts (such as bad guiding) our reduction technique is much simpler than that described in Nather et al. (1990). We simply remove parts of the light curve strongly affected by cloud, divide by the (combination of) reference stars and apply a low order polynomial fit to remove any residual trends.

3.2 Abilities of Argos

When a new instrument is commissioned, it is important to test its light gathering capabilities to ascertain the limits of where useful data can be taken. This process is still on-going with Argos.

One useful test is to measure the root mean square (rms) scatter of an object. For a star of constant magnitude, the measured brightness of the star should remain constant to within the photon noise. However, for fainter stars, difficulty in subtracting the (noisy) sky means this limit is rarely reached. The

rms scatter is a simple measure of how much a light curve from a constant star deviates from a constant value. The rms is given by

$$rms = \sqrt{\frac{\Sigma(f_i - \bar{f})}{N}} \tag{3.1}$$

where f_i is the flux in counts of the i^{th} integration, $\bar{f}$ is the mean counts, and N is the number of exposures.

To test the rms scatter of Argos, a sample of known non-pulsators of different magnitudes was examined at different integrations times [1] and the rms scatter calculated. The results are shown in Fig 3.1. It is worth noting that except for high precision photometry, accuracies of 1% are usually aimed for, and even without flat fielding our frames Argos can approach this limit for even the faintest stars we observe in reasonable exposure times.

[1]The stars were not re-observed with different exposure times, but after the frames were extracted and reduced, the counts for the star in a successive frames were co-added to give the same counts (and errors) as a longer exposure. This method is used later in the Preliminary Analysis section as well

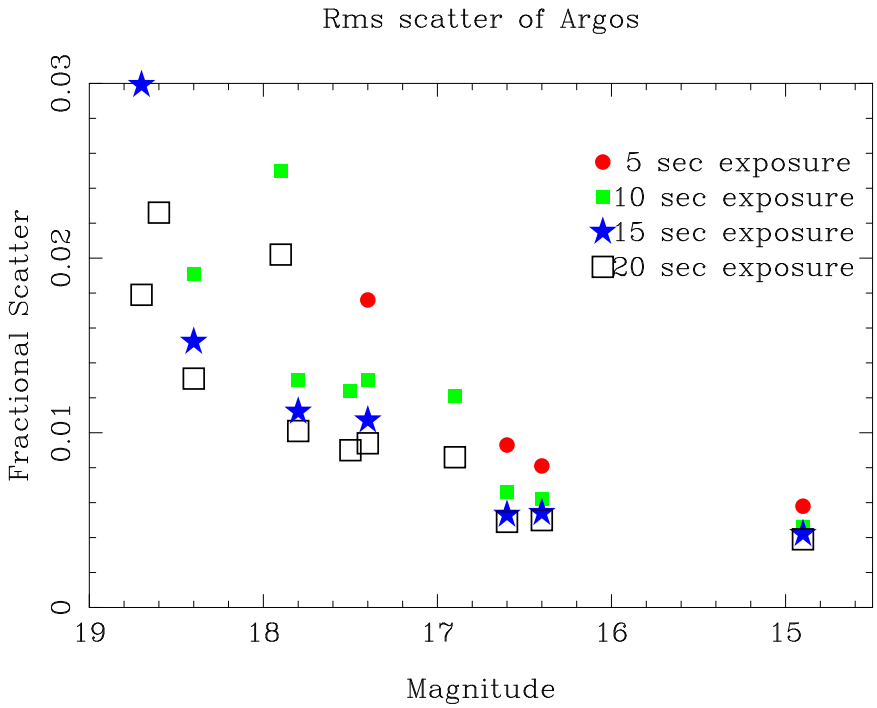

Figure 3.1 Plot of fractional scatter of observations of stars of different magnitudes. A fractional rms of 0.01 = 1%. A clear trend of increasing scatter for dimmer objects can be seen. It is also clear that long exposure times for bright objects does little to reduce the scatter, but result in a significant improvement at higher magnitudes. This plot can be used to decide the optimal exposure time on an object. It should be noted that these stars were selected because they were observed in good conditions, and scatter will be worse than shown on less photometric nights. This decision was made in the interests of consistency, it is easier to find a set of good nights, than a set of equivalently bad nights.

3.3 Preliminary Analysis

Although it is too soon to search for planets around the recently discovered variables, we can begin to analyze the data we have got so far. In particular, we can examine how the uncertainty in period decreases as we collect more data. To this end, we will look at two sample stars.

3.3.1 WD1354+0108

WD1354+0108 has a magnitude of 16.4, an amplitude of $\approx 0.6\%$ and a period of 198 seconds. As such is represents one of our brightest pulsators, but also one of the lowest amplitudes.

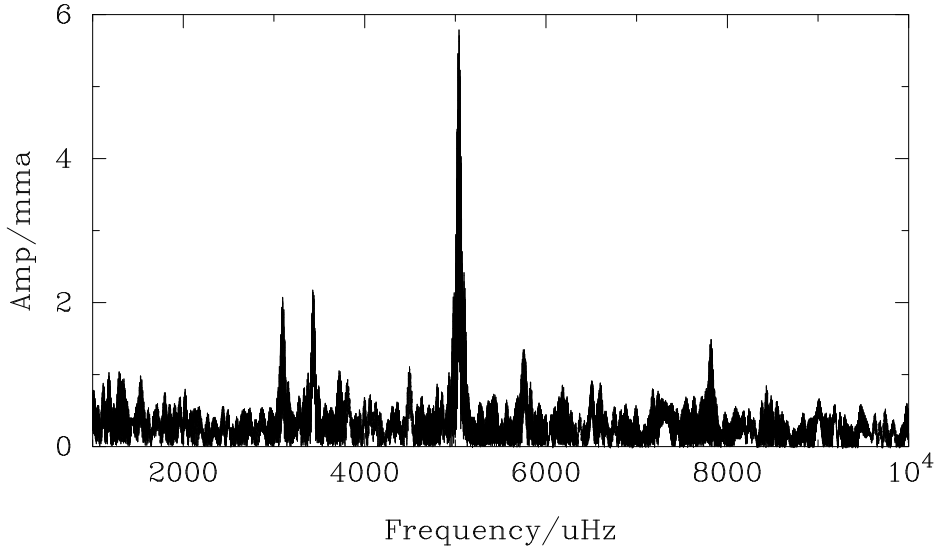

Figure 3.2 Fourier Transform of WD1354+0108 showing the dominant mode at 5000μHz. At least four smaller modes can be seen as well.

In order to accurately measure the phase of a pulsation mode we need to know the period of pulsation to a high accuracy. To measure the period of

Run	Date (UTC)	Start Time	Run Length	Exposure Time
A0577	2003-03-23	05:35:12	7 hours	5 seconds
A0580	2003-03-24	06:59:51	3 hours	5 seconds
A0598	2003-03-30	07:06:26	2 hours	5 seconds
A0629	2003-05-02	05:24:59	3 hours	5 seconds
A0639	2003-05-07	04:55:52	10 mins	5 seconds
A0640	2003-05-07	05:06:52	3 hours	5 seconds

Table 3.1 Observation log for WD1354+0108

pulsation, we need a long baseline of observations. For various reasons it is not practical or desirable to observe a single star continuously for a week or more. However, we can allow for gaps in our light curve as long as the gaps are sufficiently small.

We define a gap as sufficiently small when the uncertainty in our epoch (i.e the number of cycles of pulsation within the gap) due to the uncertainty in our period is less than 0.1. We measure our periods with a non-linear least squares fitting program, applying the equation

$$f(t) = A + Bt + C\sin\omega(t - t_0) \tag{3.2}$$

to the data, where $f(t)$ is the flux from the star at time t, and A, B, C and ω are tunable parameters. For WD1354+0108 a seven hour run (A0577), gave us a period measurement of $198.36 \pm .08$ seconds, meaning we could safely allow gaps in our light curve of up to 24 hours. A0580 lies within that period, so we can safely join these two curves together to more accurately measure the period with a significantly extended baseline.

Our measurement of the period from these two runs is $198.268 \pm .007$s and we can now safely allow a gap of 19 days.

Adding in a third run a week later gives a period of $198.239 \pm .002$s. This allows us to add data from the next run a month later. Following the same procedure as before we measure a period of $198.2385 \pm .00015$s.

As we continue to increase our baseline of observations on this star the accuracy of the period measurements will improve. When we can increase our period accuracy by another order of magnitude we expect to be able to measure the phase of the pulsations in any given run with an accuracy of order one second. At this stage we will be able to search for the phase drift characteristic of an orbiting planet.

To get the most accurate period and phase measurements we desire many data points with good signal to noise. We can increase the number of data points by taking very short exposure times, but longer exposure times give better signal to noise. To investigate whether there is an optimal exposure time, we re-did the above calculation for 10 and 20 second integrations. As Table 3.3 and Fig 3.3 show, there is no significant difference between the different exposure times, although the 5 second integrations do show a slight improvement over the longer exposures.

3.3.2 WD1345−0055

WD1345-0055 is a 16.7^{th} magnitude HDAV with a dominant mode of pulsation of about 1% at a period of 195 seconds. As can be seen by comparing Fig 3.4 to Fig 3.2, this star is very similar to WD1354+0108 being only slightly dimmer and having slightly larger amplitudes. The same process as was described above was applied to this star to determine it's period, and the results are shown in Table 3.4 and Fig 3.5.

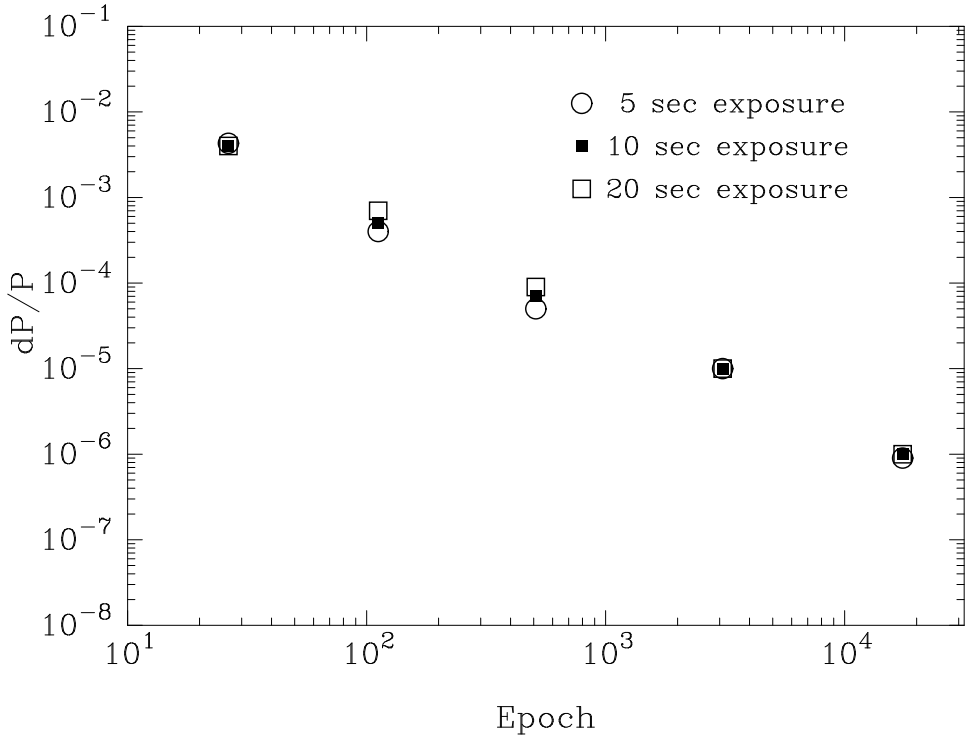

Figure 3.3 A plot of the decrease in uncertainty in the period measurement of WD1354+0108 with increasing baseline. The different symbols represent different exposure times, and it can be seen that there is little if any difference in the different exposure times used.

Run	Date (UTC)	Start Time	Run Length	Exposure Time
A0631	2003-05-03	03:03:00	7 hours	10 seconds
A0646	2003-05-09	06:04:12	3 hours	10 seconds
A0648	2003-05-10	03:02:25	5 hours	10 seconds
A0654	2003-05-12	07:32:21	1 hour	10 seconds
A0660	2003-06-29	03:02:28	1 hour	10 seconds

Table 3.2 Observation log for WD1345−0055

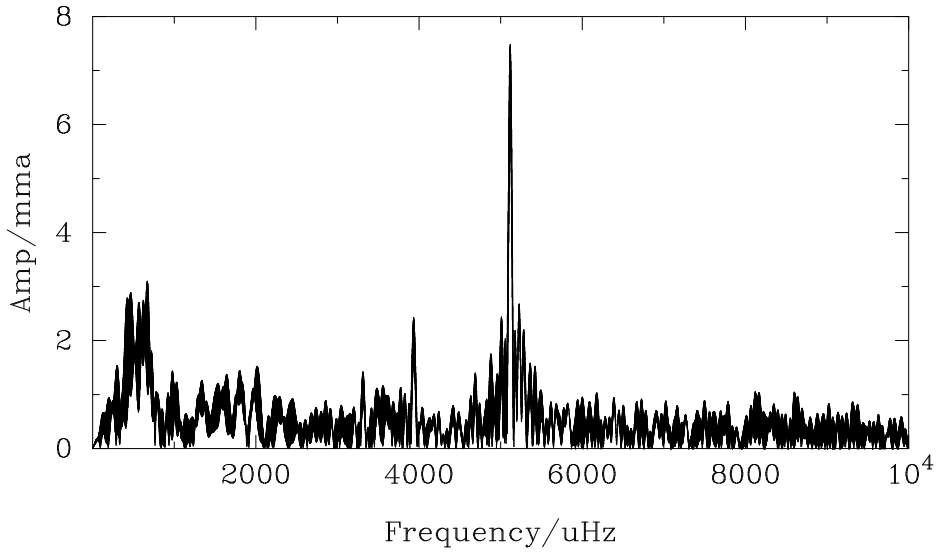

Figure 3.4 Amplitude Spectrum of WD1345-0055, showing a central peak just above 5000μHz, or 195 seconds. The amplitudes are in mma, where 8mma is equal to 0.8% change in flux. One smaller peak can be seen at 4000μHz and there may be a smaller peak at 5250μHz but it is hidden by the window function of the dominant mode.

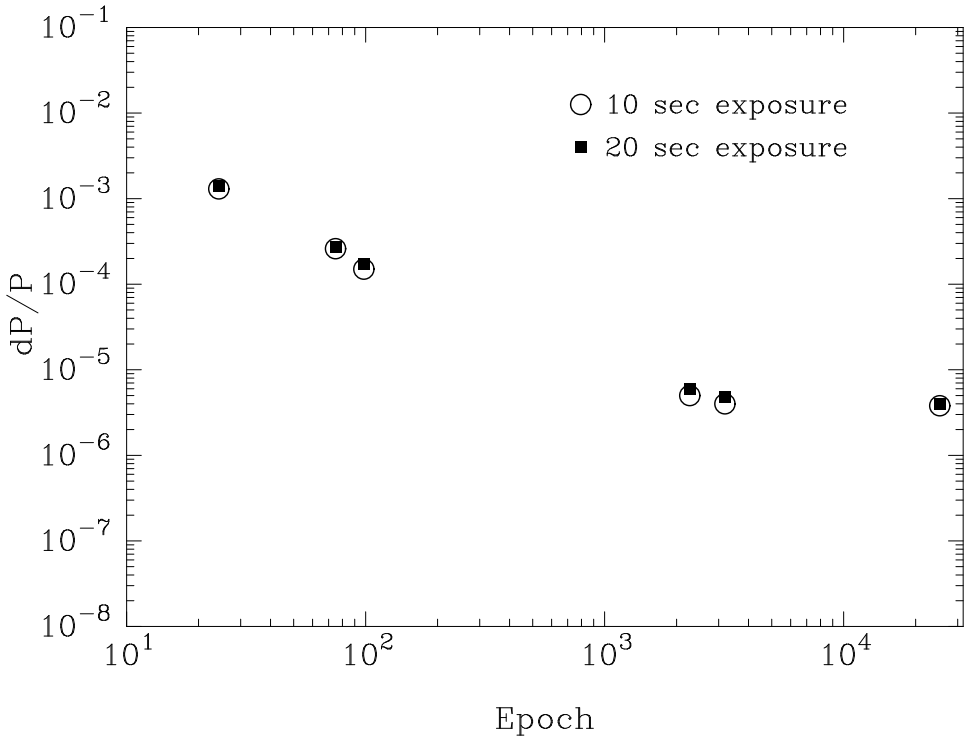

Figure 3.5 A plot of the decrease in uncertainty in the period measurement of WD1345-0055 with increasing baseline. The different symbols represent different exposure times, and it can be seen that there is little if any difference in the different exposure times used. The reason for the large error in the last data point isn't known, but a timing error cannot be ruled out.

Runs	Baseline	Epochs	5 sec P	5 sec ΔP	5 sec $\frac{\Delta P}{P}$	10 sec P	10 sec ΔP	10 sec $\frac{\Delta P}{P}$	20 sec P	20 sec ΔP	20 sec $\frac{\Delta P}{P}$
A0577a	5235	26.4	197.83	.87	4×10^{-3}	197.94	.84	4×10^{-3}	198.14	.81	4×10^{-3}
A0577	22166	111.8	198.36	.08	4×10^{-4}	198.36	.10	5×10^{-4}	198.37	.14	7×10^{-4}
+A0580	101198	510.3	198.27	.01	5×10^{-5}	198.275	.013	7×10^{-5}	198.276	.017	9×10^{-5}
+A0598	612181	3087	198.239	.002	1×10^{-5}	198.239	.002	1×10^{-5}	198.239	.002	1×10^{-5}
+A0629	3465633	17476	198.2387	.00017	9×10^{-7}	198.2388	.0002	1×10^{-6}	198.2388	.0003	1×10^{-6}
+A0639 +A0640	3980660	200731	198.2385	.00015	8×10^{-7}	198.2385	.0002	1×10^{-6}	198.2385	.0002	1×10^{-6}

Table 3.3 Period Measurement of WD1354+0108. The periods, errors and baselines are given in seconds. Baseline is the amount of time, in seconds, between the start of the first run and the end of the last run. Epochs are the number of cycles of the 198 second mode that have been completed in that baseline. The plus sign indicates that this run was added to to total amount of previous data. A0577a is the first 90 minutes of run A0577. It can be seen that 5 second exposures give marginally better error estimates than longer exposures do. True errors are probably larger than the formal errors quoted (Winget et al., 1985)

Runs	Baseline	Epochs	10 sec P	10 sec ΔP	10 sec $\frac{\Delta P}{P}$	20 sec P	20 sec ΔP	20 sec $\frac{\Delta P}{P}$
A0631a	4750	24.3	194.6	.3	1×10^{-3}	194.5	.3	1×10^{-3}
A0631b	14620	74.8	195.34	.05	3×10^{-4}	195.34	.05	3×10^{-4}
A0631	19190	98.3	195.31	.03	2×10^{-4}	195.31	.03	2×10^{-4}
+A0646	541079	2271	195.330	.001	5×10^{-6}	195.338	.001	6×10^{-6}
+A0648	622157	3186	195.335	.00085	4×10^{-6}	195.335	.00094	5×10^{-6}
+A0654 +A0660	4927959	25237	195.3350	.00075	1×10^{-6}	195.3350	.00078	4×10^{-6}

Table 3.4 Period Measurement of WD1345-0055. A0631a & b are small portions of run A0631.

3.4 Analysis of Archival Data

Of the previously known HDAVs, two (R548 and G117-B15A) have been extensively observed since their discovery nearly 3 decades ago. Although this data suffers from significantly lower signal to noise than data taken with Argos, we can still use it to place interesting limits on planetary companions for these two stars.

3.4.1 G117-B15A

We take data previously presented by Kepler et al. (2000) spanning a range of dates from the star's discovery in 1976 to the present day. This data is plotted in Fig 3.6. G117 has an amplitude spectrum very similar to WD1354+0108, with a single mode of 2%, and a handful of much smaller modes. The parabolic increase in the value of O-C is caused by the cooling of the star, which Kepler et al. (2000) measured for the first time.

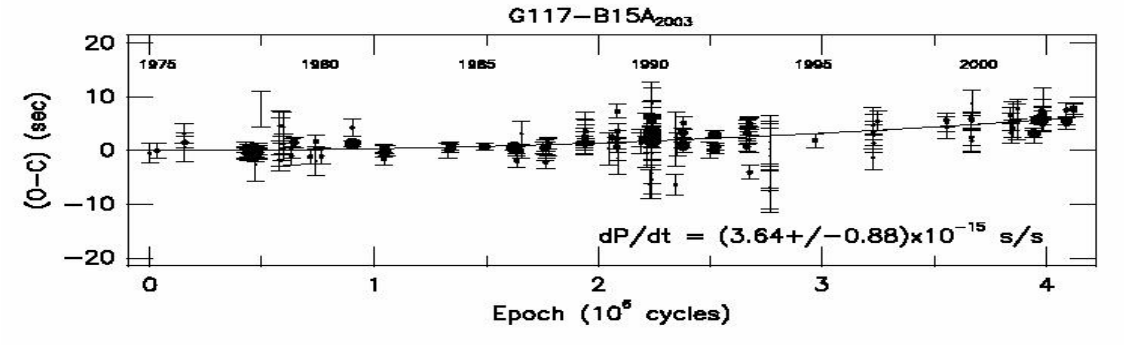

Figure 3.6 O-C diagram for the 215s pulsation of G117-B15A, taken from Kepler et al. (2000). We show 2 σ error bars on each point, and the line shows the best fit parabola to the data.

Subtracting off the best fit parabola, we take a Fourier transform of

the data, which is shown in Fig 3.7. We get a number of peaks in this plot, however as we can not fit a periodic function characteristic of a planet in an elliptical orbit to the major one we conclude that they are merely noise. We use this diagram to place a 1σ limit on the presence of short period planets. From the measurement of $\dot{P}$ we can place an lower limit on any long period planets around this star, if they exist they must be producing a period drift less than what is being produced by cooling.

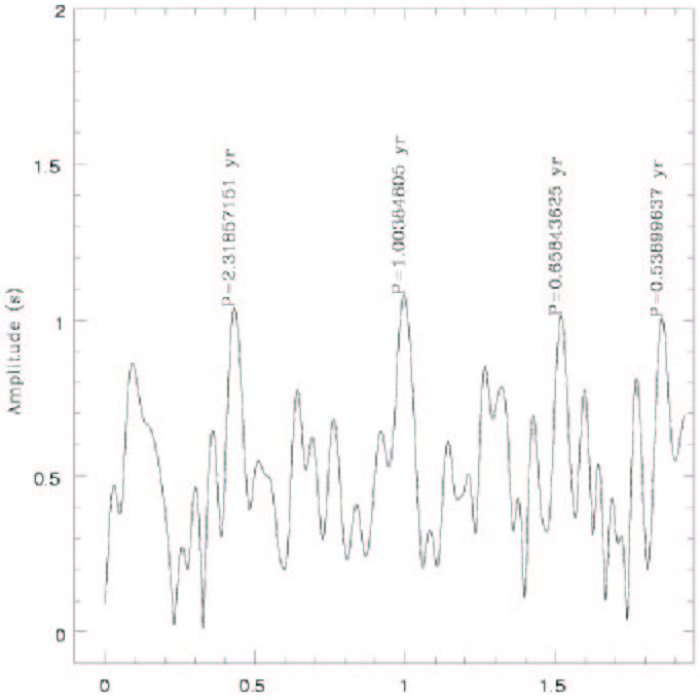

Figure 3.7 Fourier transform of O-C data for G117-B15A. Plot courtesy of S. O. Kepler

3.4.2 R548

The same procedure as outlined above was repeated for R548. R548 has a multiplet structure (see Mukadam et al. (2003a) for further details) and considerably less data than G117, as can be seen in the O-C diagram in Fig 3.8.

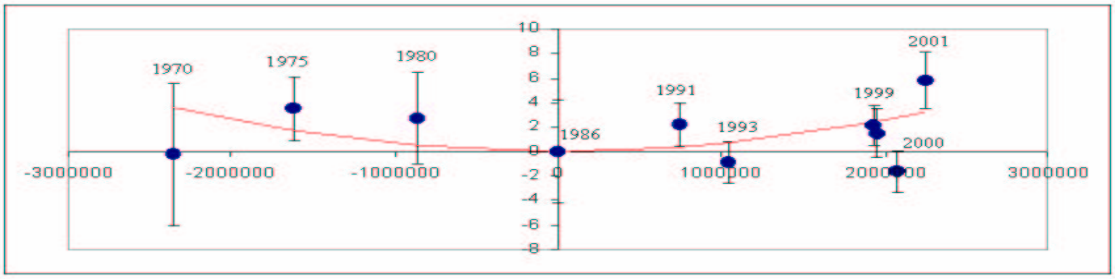

Figure 3.8 O-C diagram for R548. Data courtesy of A. Mukadam and reproduced in Mukadam et al. (2003a)

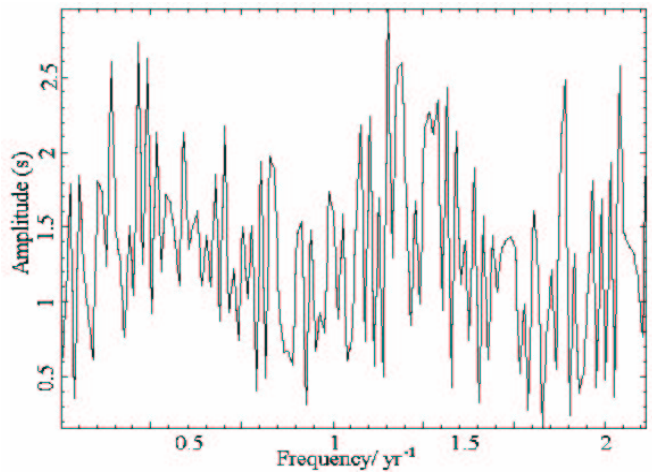

Figure 3.9 Fourier transform of O-C data for R548.

3.4.3 Planet Limits

Taking this data we can construct a plot showing what planets aren't in these systems, similar to Fig 1.3, which is shown in Fig 3.10. It is worth noting that these limits took nearly 30 years to achieve previously, but with a better instrument and a dedicated observing regime, we hope to reach these limits in approximately 3 years.

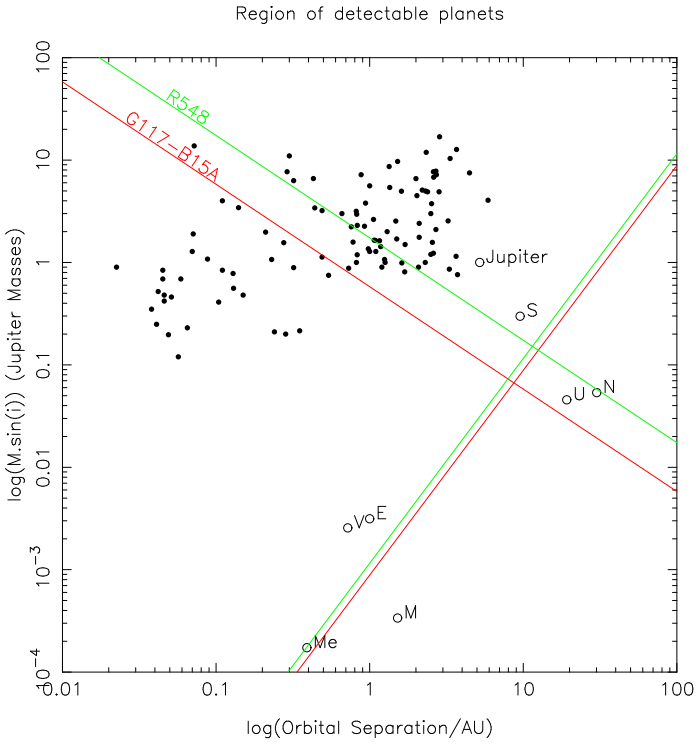

Figure 3.10 Planet limits for G117-B15A and R548. The wedge shape above the lines is the region of parameter space which does not contain a planets, or if one exists is orbits at such a high inclination to our line of sight that it can't be detected. An analogue of Jupiter or Saturn does not exist around these stars.

Chapter 4

Conclusion

The search for planets around other stars is one which has seen sizeable interest in the astronomical and general community since the first discovery of a planet around 51 Peg. The search for planets around other stars is the first step towards determining the existence and frequency of life elsewhere in the universe. HDAVs are an extraordinarily stable pulsating white dwarf, which provide an ideal opportunity to search for planets with the sensitivity of the radial velocity method but at larger orbital separations. This is astrophysically interesting because at radii where giant planets are expected to form, the radial velocity method begins to lose the sensitivity to detect planets with Jupiter masses and below.

The chief advantage of HDAVs is that monitoring the change in arrival time of the pulsations means the measured effect of a planet increases as with the orbital separation of planet and star. The existence of planets with large orbits can be ruled out in much less than the time taken to complete a single orbit by measuring the period drift caused by the acceleration of the star as it orbits the centre of mass of the planet star system.

In order to search a statistically significant number of stars for planetary systems, we are in the process of increasing the number of HDAVs known from 8 to over 30. At time of writing we have discovered 14 HDAVs bringing the number known to 22. We have demonstrated that we can find stable mode

pulsating WDs by examining the spectra of candidate objects supplied by the Sloan Survey. However, we will have to devise some method of finding these pulsators based on broad band colour information if we are to find hundreds of HDAVs, as the Sloan only provides spectra for a fraction of the objects it observes.

Although we expect planets to survive the red giant phase of the star's evolution, a null result in this search will have implications for our understanding of post main sequence evolution in stars, as well as the future of our own solar system. Regardless of the success of the planet search, our intensive observations of these stable pulsators and the resultant measurement of the period drift will reduce the uncertainties in the cooling time of WDs, improving the error on the white dwarf cosmochronological age of the Galaxy.

Bibliography

Bergeron, P., Leggett, S. K., & Ruiz, M. T. 2001, ApJS, 133, 413

Bergeron, P., Wesemael, F., Lamontagne, R., Fontaine, G., Saffer, R. A., & Allard, N. F. 1995, ApJ, 449, 258

Bevington, P. R. 1969, Data reduction and error analysis for the physical sciences, 2nd edn. (New York: McGraw-Hill, 1969)

Boss, A. P. 1995, Science, 267, 360

Bradley, P. A. 1993, Baltic Astronomy, 2, 545

Burleigh, M. R., Clarke, F. J., & Hodgkin, S. T. 2002, MNRAS, 331, L41

Debes, J. H. & Sigurdsson, S. 2002, ApJ, 572, 556

Duncan, M. J. & Lissauer, J. J. 1998, Icarus, 134, 303

Fan, X. 1999, AJ, 117, 2528

Fontaine, G., Bergeron, P., Billères, M., & Charpinet, S. 2003, ApJ, 591, 1184

Fontaine, G., Bergeron, P., Brassard, P., Billères, M., & Charpinet, S. 2001, ApJ, 557, 792

Fontaine, G., Bergeron, P., Lacombe, P., Lamontagne, R., & Talon, A. 1985, AJ, 90, 1094

Fontaine, G., Lacombe, P., McGraw, J. T., Dearborn, D. S. P., & Gustafson, J. 1982, ApJ, 258, 651

Frink, S., Mitchell, D. S., Quirrenbach, A., Fischer, D. A., Marcy, G. W., & Butler, R. P. 2002, ApJ, 576, 478

Fukugita, M., Ichikawa, T., & Gunn, J. E. e. 1996, AJ, 111, 1748

Greenstein, J. L. 1982, ApJ, 258, 661

Gunn, J. E., Carr, M., & Rockosi, e. 1998, AJ, 116, 3040

Hogg, D. W., Finkbeiner, D. P., Schlegel, D. J., & Gunn, J. E. 2001, AJ, 122, 2129

Homeier, D., Koester, D., & Hagen, H.-J. e. 1998, A&A, 338, 563

Kepler, S. O., Mukadam, A., Winget, D. E., Nather, R. E., Metcalfe, T. S., Reed, M. D., Kawaler, S. D., & Bradley, P. A. 2000, ApJ, 534, L185

Kepler, S. O., Winget, D. E., Nather, R. E., Bradley, P. A., Grauer, A. D., Fontaine, G., Bergeron, P., Vauclair, G., Claver, C. F., Marar, T. M. K., Seetha, S., Ashoka, B. N., Mazeh, T., Leibowitz, E., Dolez, N., Chevreton, M., Barstow, M. A., Clemens, J. C., Kleinman, S. J., Sansom, A. E., Tweedy, R. W., Kanaan, A., Hine, B. P., Provencal, J. L., Wesemael, F., Wood, M. A., Brassard, P., Solheim, J.-E., & Emanuelsen, P.-I. 1991, ApJ, 378, L45

Kleinman, S. J., Nather, R. E., & Phillips, T. 1996, PASP, 108, 356

Koester, D., Allard, N. F., & Vauclair, G. 1994, A&A, 291, L9

Landolt, A. U. 1968, ApJ, 153, 151

Lineweaver, C. & Grether, D. 2003, astroph/0306524

Livio, M. & Soker, N. 1984, MNRAS, 208, 763

Mayor, M. & Queloz, D. 1995, Nature, 378, 355

McGraw, J. T., Fontaine, G., Lacombe, P., Dearborn, D. S. P., Gustafson, J., & Starrfield, S. G. 1981, ApJ, 250, 349

Mestel, L. 1952, MNRAS, 112, 583

Mukadam, A., Mullally, F., Nather, R. E., & Winget, D. E. 2003c, ApJ, in prep

Mukadam, A. S., Kepler, S. O., Winget, D. E., Nather, R. E., Kilic, M., Mullally, F., von Hippel, T., Kleinman, S. J., Nitta, A., Guzik, J. A., Bradley, P. A., Matthews, J., Sekiguchi, K., Sullivan, D. J., Sullivan, T., Shobbrook, R. R., Birch, P., Jiang, X. J., Xu, D. W., Joshi, S., Ashoka, B. N., Ibbetson, P., Leibowitz, E., Ofek, E. O., Meištas, E. G., Janulis, R., Ališauskas, D., Kalytis, R., Handler, G., Kilkenny, D., O'Donoghue, D., Kurtz, D. W., Müller, M., Moskalik, P., Ogoza, W., Zoa, S., Krzesiński, J., Johannessen, F., Gonzalez-Perez, J. M., Solheim, J.-E., Silvotti, R., Bernabei, S., Vauclair, G., Dolez, N., Fu, J. N., Chevreton, M., Manteiga, M., Suárez, O., Ulla, A., Cunha, M. S., Metcalfe, T. S., Kanaan, A., Fraga, L., Costa, A. F. M., Giovannini, O., Fontaine, G., Bergeron, P., O'Brien, M. S., Sanwal, D., Wood, M. A., Ahrens, T. J., Silvestri, N., Klumpe, E. W., Kawaler, S. D., Riddle, R., Reed, M. D., & Watson, T. K. 2003a, Baltic Astronomy, 12, 71

Mullally, F., Mukadam, A., Winget, D. E., Nather, R. E., & Kepler, S. O. 2003, in White Dwarfs, proceedings of the conference held at the Astronomical Observatory of Capodimonte, Napoli, Italy. http://www.na.astro.it/meetings/wd2002/wd.html. To be published by Kluwer. (NATO Science Series II – Mathematics, Physics and Chemistry, Vol. 105, p. 337.), 337–+

Nather, R. E. & Mukadam, A. 2003, PASP, in prep

Nather, R. E., Winget, D. E., Clemens, J. C., Hansen, C. J., & Hine, B. P. 1990, ApJ, 361, 309

Pier, J. R., Munn, J. A., & Hindsley, R. B. e. 2003, AJ, 125, 1559

Rasio, F. A., Tout, C. A., Lubow, S. H., & Livio, M. 1996, ApJ, 470, 1187

Richer, H. B. & Ulrych, T. J. 1974, ApJ, 192, 719

Sion, E. M., Greenstein, J. L., Landstreet, J. D., Liebert, J., Shipman, H. L., & Wegner, G. A. 1983, ApJ, 269, 253

Smith, J. A., Tucker, D. L., & Kent, e. 2002, AJ, 123, 2121

Soker, N. 1994, PASP, 106, 59

Winget, D. E. 1998, Journal of the Physics of Condensed Matter, 10, 11247

Winget, D. E., Hansen, C. J., Liebert, J., van Horn, H. M., Fontaine, G., Nather, R. E., Kepler, S. O., & Lamb, D. Q. 1987, ApJ, 315, L77

Winget, D. E., Robinson, E. L., Nather, R. E., Kepler, S. O., & Odonoghue, D. 1985, ApJ, 292, 606

York, D. G., Adelman, J., & Anderson, J. E. e. 2000, AJ, 120, 1579

Zuckerman, B. & Becklin, E. E. 1987, Nature, 330, 138

Vita

Fergal Mullally was born in Dublin, Ireland 1 May 1979, the son of Paul and Maeve Mullally. He completed Leaving Certificate at Col*á*iste *É*anna in 1997, before reading Science at the University College Dublin. In October 2001, he graduated with Second Class Honours from the Experimental and Mathematical Physics Departments. He immediately entered the graduate school at the University of Texas and currently considers McDonald Observatory to be his home.

Someday he hopes to learn something new.

Permanent address: 11 Ashton Grove,
Dublin 16,
Ireland.

This thesis was typeset with LaTeX[†] by the author.

[†]LaTeX is a document preparation system developed by Leslie Lamport as a special version of Donald Knuth's TeX Program.